7.11 Soft Lithographic Approaches to Nanofabrication

DJ Lipomi, RV Martinez, L Cademartiri, and GM Whitesides, Harvard University, Cambridge, MA, USA

7.11.1 Introduction

7.11.1.1 Nanofabrication

Nanofabrication is the collection of techniques that generates reproducible patterns whose elements have sizes of 100 nm or less in at least one dimension.[1] The majority of commercial nanofabrication takes place in the semiconductor industry. Essentially all integrated circuits are made by a combination of electron-beam lithography (EBL), which generates nanoscale information in the form of features on photomasks, and photolithography, which replicates that information.[2] We refer to these techniques as 'conventional' methods of nanofabrication. They are the workhorses of modern microelectronics, and are not likely to be replaced in the foreseeable future. Despite the ubiquity of scanning beam and photolithographic methods in commercial production, there are many circumstances outside of microelectronics where conventional techniques are prohibitively expensive, unavailable, or inapplicable. Further, processes developed for manufacturing of microelectronics are limited to the direct patterning of resist materials on planar, rigid substrates, and are often incompatible with emerging technologies that involve unconventional and soft materials[3] and compliant substrates.[4]

There are several areas of nanoscience that demand novel approaches to nanofabrication. For example, new applications in chemistry,[5,6] biology,[7–10] medicine,[11] catalysis,[12] plasmonics,[13–15] organic electronics,[3] and materials for the conversion and storage of energy,[16–18] devices in which cost and convenience (particularly in academic research, or devices for resource-poor settings), rather than state-of-the-art performance, is the goal.[19] In addition, the ability to pattern materials that require the combination of 'top-down' fabrication with 'bottom-up' processes[20] (e.g., templated growth of crystals[21]) and self-assembly (e.g., controlling the structures formed by block copolymers[22]) also motivates researchers concerned with developing tools for forming nanoscale patterns.

7.11.1.2 Soft Lithography and Unconventional Nanofabrication

The most common forms of soft lithography use polymeric (usually elastomeric) stamps bearing relief features to transfer patterns.[23,24] The principal modes of transfer using elastomeric stamps involve printing,[25–27] molding,[28,29] phase-shifting optical lithography using conformable, transparent photomasks,[30–33] and mechanical sectioning with an ultramicrotome (nanoskiving).[34,35] Processes that form patterns by polymerization templated by a hard master are also usually included under 'soft lithography'. These methods are alternatives to replication by photolithography, and are a part of a group of techniques referred to as 'unconventional approaches' to nanofabrication.[36] A common characteristic of these approaches is their reliance on physical contact of the stamp, probe, or knife with the substrate. Physical contact – as opposed to beams of photons or charged particles – is the key mediator of pattern transfer, whose resolution is not subject to scattering and diffraction, and is, in principle, limited only by van der Waals contact and the inherent atomic and molecular granularity of matter. Along with their practical advantages, unconventional methods intrigue us conceptually because there is a potential to discover 'nano' in new and often unexpected sources. Cracks,[37] lattice steps on crystals,[38–42] shadows,[43] thin films,[44] cross sections,[45] sidewalls,[46] borders,[47,48] the cleaved edges of multilayered films,[49–52] and other discontinuities[53–55] have all been exploited to generate nanoscale information.

As soft lithography developed over the past 15 years, the areas in which it is likely to have the greatest impact are shifting. One of the principal reasons for developing soft lithography, for example, was to drive down the feature size and cost of microelectronic devices.[23] It is now clear, however, that the fabrication of deep subnanometer semiconductor devices was not the problem for which soft lithography was the most immediate solution,[5] although step-and-flash imprint lithography (SFIL) is a very promising approach to certain problems in electronic nanostructures.[56] What has emerged instead are applications in fields as disparate as cell biology[9,57] and photovoltaics.[17,58] Invention and development of new tools of fabrication at the scale of 10 nm–100 μm have also led to the creation or proliferation of new subdisciplines of science and engineering. For example, rapid prototyping of polydimethylsiloxane (PDMS) devices using soft lithography has made complex microfluidic devices relatively easy to produce,[59] and has led to recent biological applications such as cell sorting[60] and DNA sequencing[61] using PCR in microdroplets,[62] for example.

7.11.1.3 Methods of Soft Lithography for Nanofabrication

Figure 1 summarizes four general methods of replicating patterns of nanoscale features using soft lithography: printing, molding, phase-shifting edge lithography, and nanoskiving. Printing and molding replicate nanoscale features directly: that is, there is a one-to-one correspondence between the dimensions

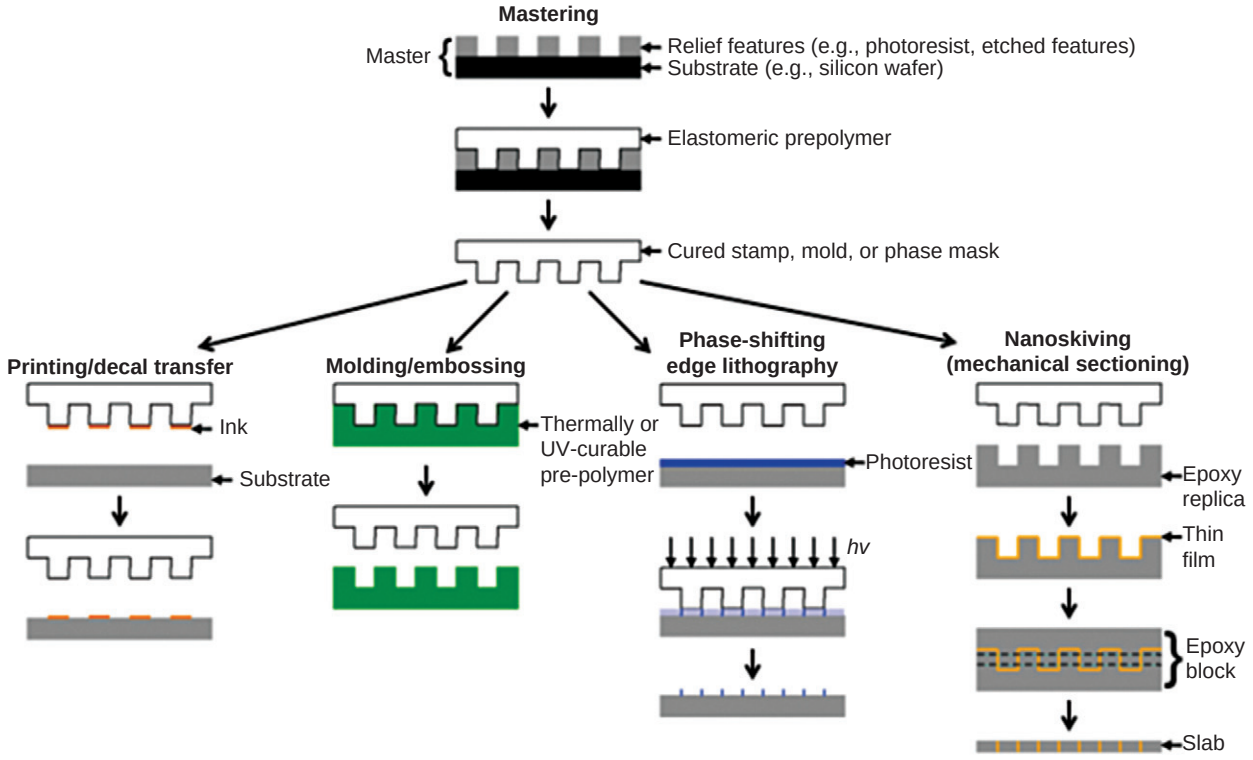

Figure 1 Overview of the four general approaches to nanofabrication by soft lithography. Mastering using lithography or another approach produces a template with topographic features, over which an elastomeric prepolymer is poured and cured. The cured slab of elastomer is an inverse replica of the master, and functions as the element of pattern transfer in the four general methods of soft lithography discussed in this chapter: (1) printing and decal transfer, in which the stamp transfers material directly to a substrate; (2) molding, in which the stamp molds another material; (3) phase-shifting edge lithography, in which the stamp behaves as a conformal optical mask, where the edges of the features are transferred to a film of photoresist; and (4) nanoskiving, in which the stamp molds an epoxy prepolymer, which is coated with thin metallic, semiconducting, dielectric, or polymeric films, embedded, and sectioned with an ultramicrotome.

of the master, the stamp, and the final pattern. They require high-resolution masters in order to transfer patterns with nanoscale lateral dimensions. Phase-shifting edge lithography and nanoskiving form patterns with nanoscale linewidths indirectly, by using edges of topographic features. The masters for these 'edge lithographic'[1] techniques can thus have features that are larger than the dimensions of the desired structures.

7.11.1.4 Objective of the Chapter

The goal of this chapter is to outline and summarize methods for nanopatterning by soft lithographic printing, molding, phase-shifting edge lithography, and nanoskiving, and to describe recent applications and developments. Chapter 7.13 by Carter reviews forms of nanoimprint lithography – replication of patterns using hard stamps – we therefore restrict our attention to techniques that use soft, polymeric stamps, but we will make a brief exception for SFIL (Section 7.11.4.3). We also will not cover scanning probe lithography (e.g., dip-pen nanolithography[63]), which, like printing with elastomeric stamps, can form patterns of many different materials on a substrate, and can operate in both serial and parallel modes.[64,65]

Unconventional approaches to nanofabrication occupy a range of stages of development. Molding using hard stamps is employed in commercial production of optical storage media (e.g., compact discs (CDs), digital versatile discs (DVDs), and Blu-ray discs), and soft methods of molding nonplanar substrates have clear potential for manufacturing. Particle replication in nonwetting templates (PRINT) has been commercialized for possible applications in drug delivery.[11] Nanoskiving is in a relatively earlier stage of development, and its primary uses are still in academia.[66] This chapter should thus appeal to researchers in a variety of disciplines who work in areas at different stages of technological development, though the newness of the selected topics probably skews the audience who will derive the most benefit toward academic scientists and engineers, and toward industrial engineers facing problems that seem intractable using photolithography.

7.11.1.5 Scope

This chapter begins by describing recent developments in materials for stamps and methods of generating topographic templates. We then identify new directions in printing, molding, phase-shifting edge lithography, and nanoskiving, by highlighting salient examples, and include techniques that are capable of fabricating three-dimensional (3D) nanostructures. While some older information is necessary to provide context, we emphasize techniques that have developed over approximately the past 5 years. The review by Xia and Whitesides provides an account of the early development of soft lithography and its applications through 1998.[23,67] The review by Xia *et al.*[36] covers unconventional nanofabrication in general through 1999, and was updated in 2005 in the review by Gates *et al.*[1] Research on unconventional nanofabrication published through 2007 appears in the review by Stewart *et al.*[68] Saavedra *et al.*[69] presents a review of hybrid strategies for nanolithography that combine conventional patterning with chemical and physical functionality enabled by intermolecular, electrostatic, or biological interactions. There are also reviews that cover specific major applications of soft lithographic patterning. The review by Menard *et al.*[3] covers patterning for organic electronic and optoelectronic systems, while the review by Stewart *et al.*[13] covers several approaches for patterning plasmonic materials.

7.11.2 Materials and Methods

7.11.2.1 Introduction

In most cases, there are two components necessary to perform soft lithography: a master and a stamp. The master is the template bearing topographic features from which the stamp is molded, as an inverse replica. There are exceptions: silicon and quartz stamps for nanoimprint lithography are usually patterned directly on the nanoscale using EBL and reactive-ion etching (RIE), and Marks and co-workers have developed a method to pattern PDMS slabs directly with EBL.[70] This section reviews methods of creating masters from which nanoscale features can be derived, and then describes materials used for stamps, with a focus on soft materials. The work of Qin *et al.*[24] provides detailed experimental protocols for mastering, production of PDMS stamps, and several forms of printing and molding.

7.11.2.2 Preparation of Masters

Conventional lithography is the most general way to prepare masters for soft lithography. The method for fabricating masters with nanoscale features (10 nm) with arbitrary geometries is EBL. It is, however, time consuming, expensive, requires significant experience, and is not accessible to all users. Photolithography can easily generate relief patterns of photoresist that can serve as templates for molding a prepolymer. Obtaining a minimum feature size of 1 μm from a chrome mask can be accomplished using ultraviolet (UV) exposure tools found in academic clean rooms. The use of printed transparency masks is, however, significantly less expensive and faster than ordering and fabricating a chrome mask, for fabricating feature sizes 8 μm.[71] Our laboratory commonly uses SU8 negative-tone photoresist for its adhesion to silicon wafers and its durability.

Direct laser writing (DLW) and multiphoton polymerization and depolymerization can produce sophisticated patterns in two or three dimensions.[72,73] Multiphoton absorption (MPA) is a serial lithographic tool that depends nonlinearly on intensity. It is thus possible to induce photochemical reactions anywhere in the focal volume of a laser beam that is passed through the objective of a microscope, and is applicable to many photosensitive materials, including organic[74] and inorganic[75,76] photoresists. True 3D structures can be produced whose characteristic voxel sizes can be smaller than a diffraction-limited spot, because the threshold of intensity that promotes the photochemical reaction may only take place in the center of the spot. The process can thus produce voxels with sizes of 100 nm when exposed using 800 nm light from a Ti:sapphire laser.[77] LaFratta *et al.*[78] have used MPA to master 3D structures using membrane-assisted microtransfer molding (MA-μTM; see Section 7.11.4.5). The most common application of MPA is to harden materials at the sites of irradiation (negative photoresists, such as SU8),[79] but can also be used to etch polymers at the sites of irradiation.[80] Ibrahim

et al.[80] surveyed the behavior of several positive-tone resists for multiphoton depolymerization, including poly(methyl methacrylate) (PMMA), polystyrene (PS), poly(butyl methacrylate) (PBMA), and poly[2-(3-thienyl)ethyloxy-4-butylsulfonate] (PTEBS), and found that the best materials had high glass transition temperatures, low molecular weights, and no visible absorption. PMMA, which absorbs 4–6 photons per reaction when irradiated with 800 nm light, produced the sharpest patterns of the materials tested, which were transferred easily to PDMS stamps.[80]

There are several nonphotolithographic methods that have been used to generate topographic patterns for soft stamps.[81] Simple patterns can be generated from commercial structures, such as blazed diffraction gratings[34] or anodic alumina membranes,[58] whose sizes of pores can be controlled electrochemically. Self-assembled systems, such as the structures produced by nanosphere lithography[81,82] and block copolymers,[83] can also be used as topographic templates. The work of Russell and co-workers,[22,70,84,85] Ruiz *et al.*,[86] Hawker and Russell,[22] and Segalman[87] have demonstrated the utility of the patterns produced by block copolymer lithography.[85] The greatest level of control in these systems is achieved by patterning the substrate topographically[87] or chemically[88] to produce hierarchical structures.[89,90]

Unconventional nonlithographic methods to produce stamps include casting the elastomeric prepolymer against cracks,[37] carbon nanotubes,[91] single cells, and proteins.[92] Grimes *et al.* demonstrated a clever rapid prototyping technique for creating masters for soft lithography. Their method is based on laser printing on pre-strained PS sheets ('shrinky-dinks').[93] Upon baking, the sheets contract laterally, and the printed features become taller. The minimum linewidth that could be achieved was 65 μm, while the thickness of the ink could be several tens of microns, depending on the amount of ink deposited by the printer.[94,95]

7.11.2.3 Materials for Stamps

The most common material used for soft lithographic stamps is PDMS, a commercially available, thermally curable, elastomeric polymer. (Our laboratory uses Sylgard 184, Dow Corning, Midland, MI.) PDMS has three properties that make it ideal for many applications. (1) It is elastic. This characteristic, combined with its low surface energy, enables it to make reversible conformal contact with non-planar substrates with minimal applied pressure to curved surfaces.[67] Treatment with an oxygen plasma, however, renders the surface of a PDMS stamp hydrophilic and reactive, such that it can form irreversible bonds with a substrate. (2) It is mostly transparent down to wavelengths of 280 nm. It can therefore be used as a mold for UV-imprint lithography.[96] (3) It is commercially available in bulk quantities ($\sim \$100\,kg^{-1}$). The moderate price of the material enables its use for rapid prototyping.

PDMS also has deficiencies. For example, it is not the best material for high-aspect-ratio structures. Mechanical stress, electrostatic attraction, and capillary forces can cause PDMS features on a stamp to self-adhere. In general, commercial Sylgard 184 works best for patterning features with sizes >100 nm.[97] Printing and molding features with sizes <100 nm require a polymeric stamp that is stiffer than Sylgard 184. Hard and stiff polymers, however, tend to be brittle, and cannot conform to surfaces as does PDMS. Variants of PDMS have been developed to improve the fidelity and resolution in soft lithography for some applications.

To replicate features smaller than 100 nm using elastomeric stamps, Michel *et al.*[98] developed a 'hard-PDMS' (h-PDMS) with a higher Young's modulus (~ 10 MPa) than PDMS (~ 0.6 MPa). There are, however, trade-offs for the high resolution of h-PDMS. For example, releasing it from the master can crack the surface of the stamp, and external pressure is required to achieve conformal contact with a substrate, which can create long-range, nonuniform distortions over the large areas of contact.[99]

One of the primary advantages conferred by elastomeric stamps is the ability to produce patterns on nonplanar substrates.[100–102] While PMDS alone has sufficient rigidity to transfer micrometer-sized features to hemispherical substrates,[28] replication of nanostructures to nonplanar substrates requires the use of a composite stamp composed of a thin, rigid layer bearing the relief features, bonded to a thicker, flexible backing of PDMS. These composite stamps often bear a layer of h-PDMS,[103] or a hard, inelastic polymer, which supports nanoscale patterns, and a flexible backing of standard PDMS.[103,104] Li *et al.* used a stamp with a thin (100–200 nm), rigid, UV-curable, and topographically patterned layer, supported by a thick (2 mm) PDMS layer. This composite stamp could replicate 15 nm features at pitch of 100 nm, and could pattern lines of resist with 100-nm half-pitch on the curved surfaces of optical fibers (see **Figure 2**).[105] Stamps comprising blended polymers can be used for applications that require hydrophilicity and elasticity,[106] and photocurability.[96,107]

Other, nonelastomeric, hard polymers that have been used for stamps include PMMA,[108,58] poly([3-mercaptopropyl] methylsiloxane) (PMMS),[109] PS,[110] and epoxy resin.[111] The use of photocurable elastomers enables low-temperature curing, and eliminates heating steps and concomitant distortion of the master and stamp.[112,113]

A class of material that has received attention over the past 5 years is the perfluoropolyethers (PFPEs).[114,115] These elastomers generally have a low Young's modulus, high gas permeability, low toxicity, and swell minimally.[116] The Teflon-like, low surface energies of stamps composed of PFPEs enable them to be used with organic solvents for microfluidics,[117] and their surfaces can be functionalized.[118] This chapter will revisit PFPEs in Section 7.11.4.4.

There is no single criterion for the 'best' material for soft lithographic stamps. Different applications require different combinations of properties. **Table 1** lists the physical properties of six of the most common polymers used in soft lithography: PDMS (h-PDMS and soft-PDMS (s-PDMS)),[116] PMMA,[108] PS,[109] and PFPE.[114]

7.11.3 Printing

7.11.3.1 Introduction

Nanofabrication by printing is the transfer of material from a topographically patterned stamp to a surface. Printing is an additive process – material is deposited only where it is required – whereas conventional lithography is subtractive – photoresist and other materials are usually discarded during spin coating and development of substrates. Microcontact de-printing is the subtractive form of microcontact printing

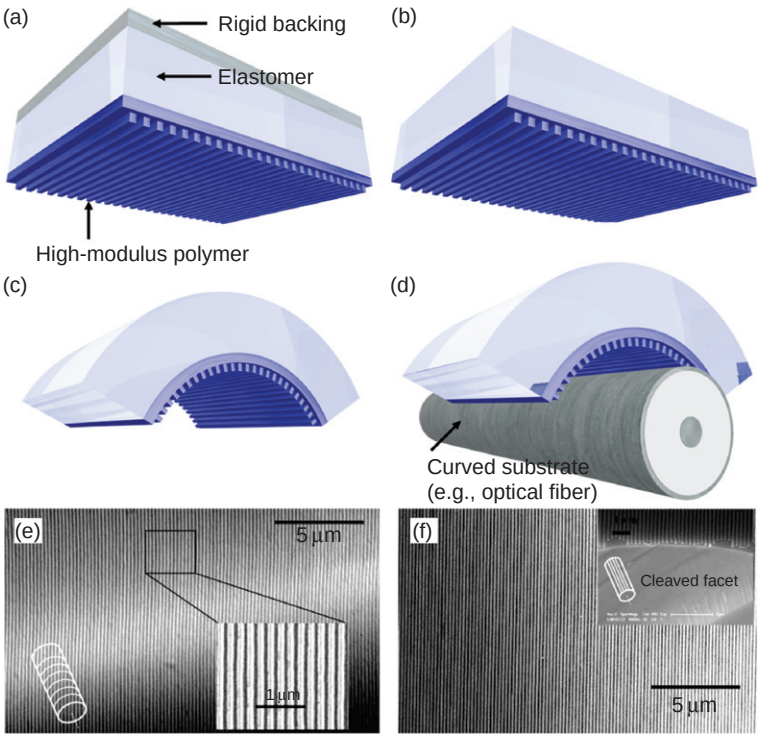

Figure 2 Schematic drawings of composite stamps and images of imprinted patterns on cylindrical substrates. (a) A three-layer stamp comprising a patterned layer of a high-modulus polymer (e.g., epoxy, PMMA, or h-PDMS), an elastomeric layer, and a rigid backing. (b) A two-layer stamp without the rigid support. This stamp can be bent (c) in order to conform to nonplanar surfaces (d). (e and f) Scanning electron microscope (SEM) image of an imprinted grating structure on the surface of an optical fiber. (e and f) Reproduced with permission from Li, Z. W.; Gu, Y. N.; Wang, L.; *et al. Nano Lett.* **2009**, *9*, 2306–2310.[105] Copyright 2009, American Chemical Society.

Table 1 Physical properties and resolutions reported for different polymers used for soft lithography

Material	*Young's modulus (MPa)*	*Surface energy (erg cm^{-2})*	*Resolution (nm)*	*Reference*
PDMS	0.6	25	250	122
h-PDMS	10.0	35	50	122
s-PDMS	0.4	15	500	122
PMMA	8000.0	750	100	110
PS	5000.0	106	100	123
PFPE	0.8	11	15	117

(μCP), in which material is removed from the substrate in the areas where the stamp makes contact.[119] This section describes recent developments in μCP,[67] including seeded growth of crystals of organic[120] and inorganic[121] semiconductors, kinetically controlled decal transfer printing,[122] and biological applications of printing.[123]

7.11.3.2 Microcontact Printing

μCP can be used to pattern alkane thiolates, silanes, biomolecules, colloidal particles, and polymers on metal and semiconductor surfaces.[67] It works by transferring material – for example, self-assembled monolayers (SAMs) of alkane thiolates on metal surfaces – directly to the substrate.[20] SAMs can be used, for example, to tune the wetting properties of surfaces and template the formation of secondary structures of another material,[120] serve as an etch resist,[25] or mimic the extracellular matrix to simulate the microenvironments of cells.[124] The lateral resolution of μCP can be < 100 nm, and it depends on the properties of the stamp and the extent to which the 'ink' diffuses across the substrate. The smallest features transferred into a metal film by selective etching were 35 nm trenches separated by 350 nm.[25] μCP is high throughput (especially when using a cylindrical, rolling stamp[26]) and is applicable to many types of materials. **Figure 3** illustrates two methods of fabricating metallic nanowires by μCP: (1) printing monolayer resists on metallic films, and etching the unprinted regions (**Figure 3(a)**); and (2) printing seeding solutions or catalysts for electroless deposition from solution (**Figure 3(b)**).[125] **Figures 3(c)–3(f)** show nanowires of gold, silver, copper, and palladium prepared by printing and etching. Overlay resolution for layered patterns can be as high as 500 nm.[126] Mechanical compression or swelling of the stamp with a solvent can cause lateral spreading of the contact area of the relief features across a surface. This action can reduce the lateral spacing between features, and can produce features with, for example, submicrometer linewidths, from a stamp with micrometer-sized features.[27] An extension of μCP is electrical-μCP, which uses a PDMS stamp coated with a metallic film to print charge into a film of a dielectric polymer, such as PMMA.[127,128] The highest resolution obtained using electrical-μCP was 100 nm. Xia and co-workers described a printing technique called 'edge-spreading lithography', in which an unpatterned stamp, inked with alkane thiols, was

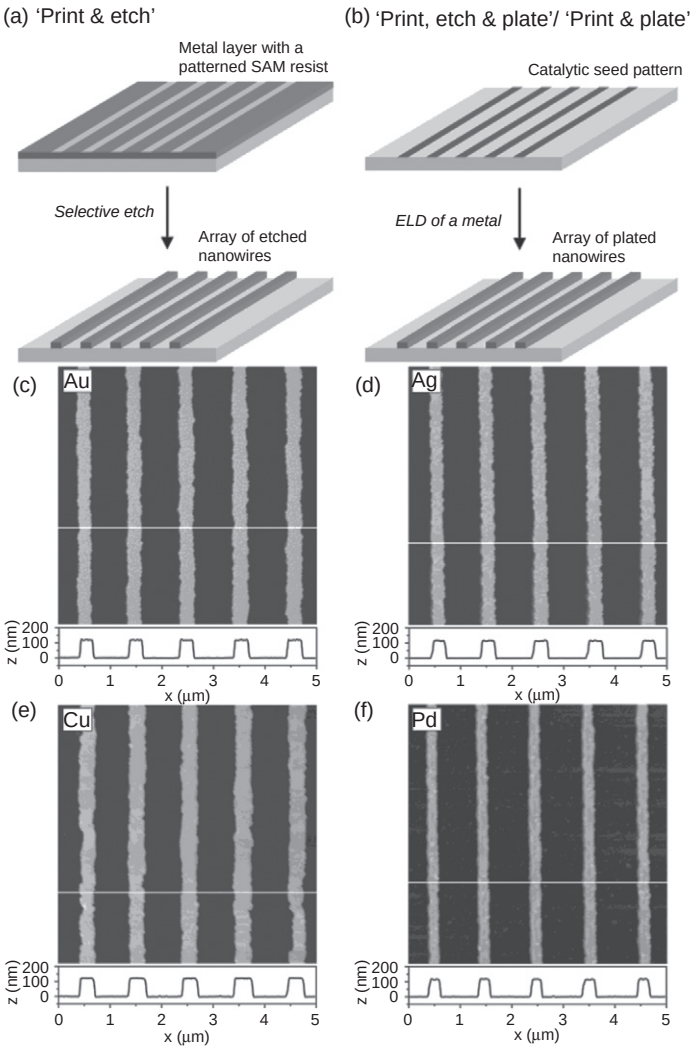

Figure 3 Use of microcontact printing to pattern nanowires of gold, silver, copper, and palladium. (a) Summary of the subtractive procedure used to print a monolayer resist on a metallic film. Subsequent etching of the unprinted areas produces nanowires defined by the printed areas. (b) Summary of the additive process used to print seeding solutions or catalysts that direct the formation of nanowires using electroless deposition (ELD). (c–f) Atomic force microscope (AFM) images of gold, silver, copper, and palladium nanowires formed by subtractive etching. Reproduced from Geissler, M.; Wolf, H.; Stutz, R.; *et al. Langmuir* **2003**, *19*, 6301–6311.[125] Copyright 2003, American Chemical Society.

brought into contact with a patterned photoresist layer on a metallic film. The thiols migrated to the metallic film around the edges of the photoresist features. Upon release of the stamp, dissolution of the photoresist features, and etching the metallic film produced metal nanowires that outlined the locations of the photoresist features.[129]

SAMs and other printed materials can be used to pattern the regions of the nucleation of different types of crystals. Aizenberg *et al.*[21] first demonstrated this principle by selective nucleation of calcite crystals in regions of a substrate covered by a monolayer presenting carboxylic acid groups. In a related approach, Briseno *et al.*[119] was able to pattern single crystals, from the vapor phase, of organic semiconductors, including C_{60}, pentacene, and rubrene, directly onto source and drain electrodes to fabricate high-performance, organic thin-film transistors on flexible substrates. Figure 4(a) shows a schematic drawing of the process used for the templated nucleation of crystals of organic semiconductors. Figures 4(b) and 4(c) show examples of arrays of crystals, and Figure 4(d) shows patterns of calcite crystals. Wang *et al.*[121] demonstrated anisotropic and patterned growth of ZnO nanocrystals by printing a seeding solution (Figures 4(e)–4(f)). Another interesting application of μCP is in area-selective atomic layer deposition (ALD) of HfO_2 and platinum for integrated circuits and fuel cells.[130] Solvent-assisted lithography is an edge-lithographic printing technique in which a solution, constrained in the void spaces between a stamp and a substrate, evaporates and leaves 'coffee rings' around the edges of the features.[131] Shi *et al.*[131] produced features with sub-100 nm linewidths from solutions of TiO_2 using this method.

7.11.3.3 Decal Transfer Printing

Decal transfer printing is the use of a stamp to transfer preformed structures directly to a substrate. The 'ink' can be metallic,[132] semiconducting,[122] or organic,[133] and can produce 2D or 3D patterns.[134] In contrast to μCP of small molecules

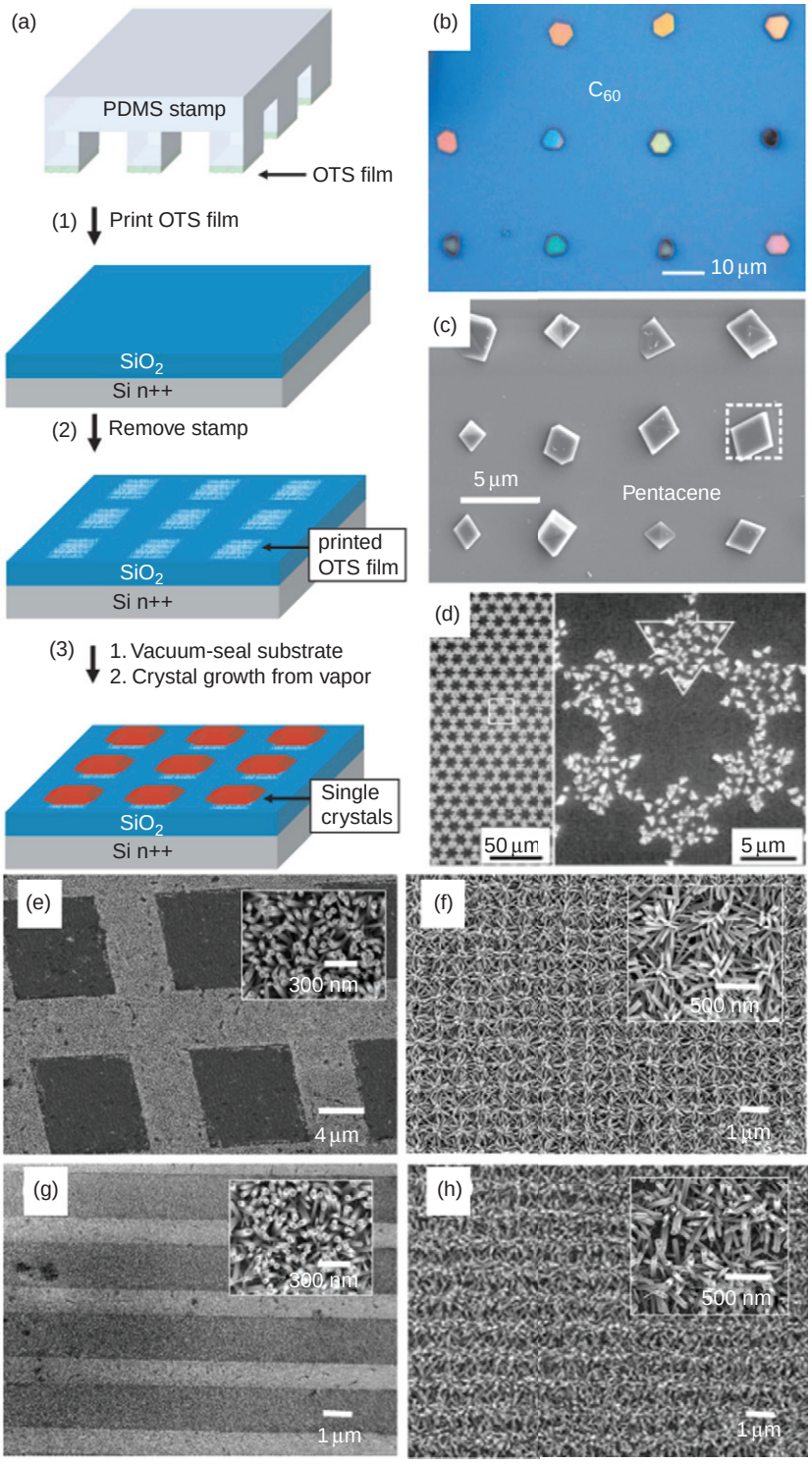

Figure 4 Patterned growth of crystals and nanowires by microcontact printing. (a) Schematic drawing of the process used to microcontact print patterns of octadecyltrichlorosilane (OTS) on a substrate. These regions nucleate the growth of single crystals of organic semiconductors from the vapor phase, such as buckminsterfullerene (C_{60}, b) and pentacene (c). The different colors arise because of the interference of white light within crystals of different thickness. Reproduced with permission from Briseno, A. L.; Mannsfeld, S. C. B.; Ling, M. M.; *et al. Nature* **2006**, *444*, 913–917.[120] Copyright 2006, Nature Publishing Group. (d) Patterns of calcite crystals on palladium. The patterns were determined by microcontact printing two types of self-assembled monolayers with different functional groups. Reproduced with permission from Aizenberg, J.; Black, A. J.; Whitesides, G. M. *Nature* **1999**, *398*, 495–498.[21] Copyright 1999, Nature Publishing Group. (e–h) Patterned nucleation of zinc oxide nanocrystals. Reproduced with permission from Wang, C. H.; Wong, A. S.; Ho, G. W. *Langmuir* **2007**, *23*, 11960–11963.[121] Copyright 2007, American Chemical Society.

where the stamp acts as a reservoir of ink,[26] in decal transfer printing, the stamp must be reloaded after every stamping operation. In some instances, the material of which the stamp is composed of can be transferred to the substrate directly. For example, Ahn *et al.*[135] have used decal transfer printing of PDMS as an etch resist in microfabrication.

When a PDMS stamp is placed in contact with solid structures on a substrate, the strength of adhesion scales with the speed with which the stamp is peeled off the substrate. This phenomenon is based on the viscoelasticity of PDMS, and allows materials to be transferred to a PDMS stamp when withdrawn quickly, and printed on another substrate when withdrawn slowly. Meitl *et al.*[122] produced patterns of many solid objects – single-crystalline silicon and gallium nitride, mica, highly oriented pyrolytic graphite, silica, and pollen. Materials that can act as receiving substrates include silicon, silica, indium phosphide, sodium chloride, magnesium oxide, and PS.[122] Figure 5(a) shows a schematic diagram of the process used to transfer structures by kinetically controlled adhesion. Figures 5(b) and 5(c) are strips of gallium nitride (Figure 3(b)) and silicon (Figure 5(b)) printed onto a Si(100) wafer.

7.11.3.4 Biological Applications of μCP

The ability to pattern surfaces with regions bearing arbitrary functional groups has important consequences for biology. The work of Kilian *et al.*,[123] Xia *et al.*,[136] and others has demonstrated the utility of μCP of SAMs to mimic the microenvironments of cells in tissue to study a variety of processes in biochemistry and cell biology.[9] For example, the ability to control the shapes of cells by patterning SAMs that mimic the extracellular matrix could lead to an understanding of the geometrical cues that govern apoptosis,[137] motility,[136] and differentiation (e.g., of stem cells).[123,138] The ability to tune the surfaces of PDMS stamps themselves could also enable improved biochemical assays. Lowe *et al.*[139] have found that PDMS stamps, presenting covalently immobilized antibodies, can be used to capture, isolate, and transfer transmembrane proteins, which are ordinarily difficult to isolate using unfunctionalized surfaces. These findings could have broad significance in biomedicine.

7.11.4 Molding

7.11.4.1 Introduction

Molding is a conceptually simple form of transferring patterns by soft lithography. A topographically patterned polymeric stamp is placed into contact with a precursor of a solid material, which can be a prepolymer, solution, or melt. Many types of materials have been molded: polymers, gels, precursors to ceramics, inorganic carbon, luminescent phosphors, salts, and colloids.[140,141] Soft lithographic molding has advanced considerably over the past 5 years in terms of both the absolute sizes and aspect ratios of features that can be replicated, and the ability to mold patterns over nonplanar substrates. Forms of molding that have been invented or significantly developed over the past 5 years are SFIL,[56] PRINT,[11] which uses a fluorinated elastomer and substrate to produce isolated nanoparticles with different shapes and compositions,[142] 3D molding, including MA-μTM,[78] micromolding in capillaries (MIMIC),[143] and solvent-assisted micromolding (SAMIM).[144] An important consideration in all forms of molding is the release of stamp from master, and replica from mold.[114]

7.11.4.2 Pushing the Limits of Molding

The resolution of molding is limited, in principle, by the inherent atomic and molecular graininess of matter and the rigidity of the mold and the material being molded. Molding cracks, crystallographic steps, and single molecules illustrate what is, so far, the ultimate resolution of soft lithographic molding. Xu *et al.*[37] replicated a crack in a silicon wafer with a step height of 0.4 nm to a polyurethane replica, using an h-PDMS mold (Figure 6), while Elhadj *et al.*[145] replicated elementary steps on ionic crystals of 0.3–0.4 nm. Rogers and co-workers have demonstrated molecular-scale resolution by replicating the shapes of single-walled carbon nanotubes in polyurethane using an h-PDMS/PDMS stamp.[91,146]

These demonstrations of the small absolute sizes replicable by molding have accompanied equally interesting demonstrations of replicating very high-aspect-ratio features. The Aizenberg laboratory has demonstrated the replication of large ($>1\,cm^2$) arrays of high-aspect-ratio epoxy nanoposts ($d = 250$ nm and $h = 8$ μm, Figures 7(a) and 7(b)),[147] which form hierarchical helical assemblies by capillary forces upon wetting by a solvent and subsequent evaporation.[148] These tentacle-like structures can be used to grasp micrometer-sized beads, and could be a component of bio-inspired functional surfaces (Figures 7(c)–7(e)).[147] The use of elastomeric molds permits deformation of the mold[27] during infiltration of the polymer, which, upon curing of the epoxy, can produce skewed, elongated, or compressed arrays of nanoposts (Figure 7(f)).[147]

7.11.4.3 Step-and-Flash Imprint Lithography

Embossing using hard molds in various forms has been used commercially on the submicrometer scale for decades in the production of CDs, DVDs, diffraction gratings, and holograms.[1] Chou and co-workers were the first to apply this approach to the fabrication of sub-100-nm structures for microelectronic applications – nanoimprint lithography[149,150] – which is reviewed in Chapter 7.13 by Carter. The most common hard molds are made from quartz, silicon, and metals, with minimum feature sizes of 20 nm for quartz and 10 nm for silicon.[1] Molds are prepared by first patterning a resist film on the flat substrate by e-beam or photolithography, and then modifying the exposed regions using RIE, wet etching, or electroplating. The use of transparent quartz molds has enabled the most successful form of nanoimprint lithography to date: SFIL.

SFIL has been developed over the past decade by Willson and co-workers:[151,152] it replaces the photomask in traditional photolithography with a quartz mold, and replaces complex optical steppers with molding tools. Figure 8(a) summarizes the procedure used. The prepolymer is irradiated and cross-linked through the transparent mold. Release of the mold reveals the relief structure in the cross-linked polymer. A residual layer ('scum') connects the molded features in the imprint resist to one another. A breakthrough etch removes the scum layer and completes the pattern transfer step. The unconnected features of imprint resist can then direct further elaboration of the substrate.[153] Figure 8(b) shows an example

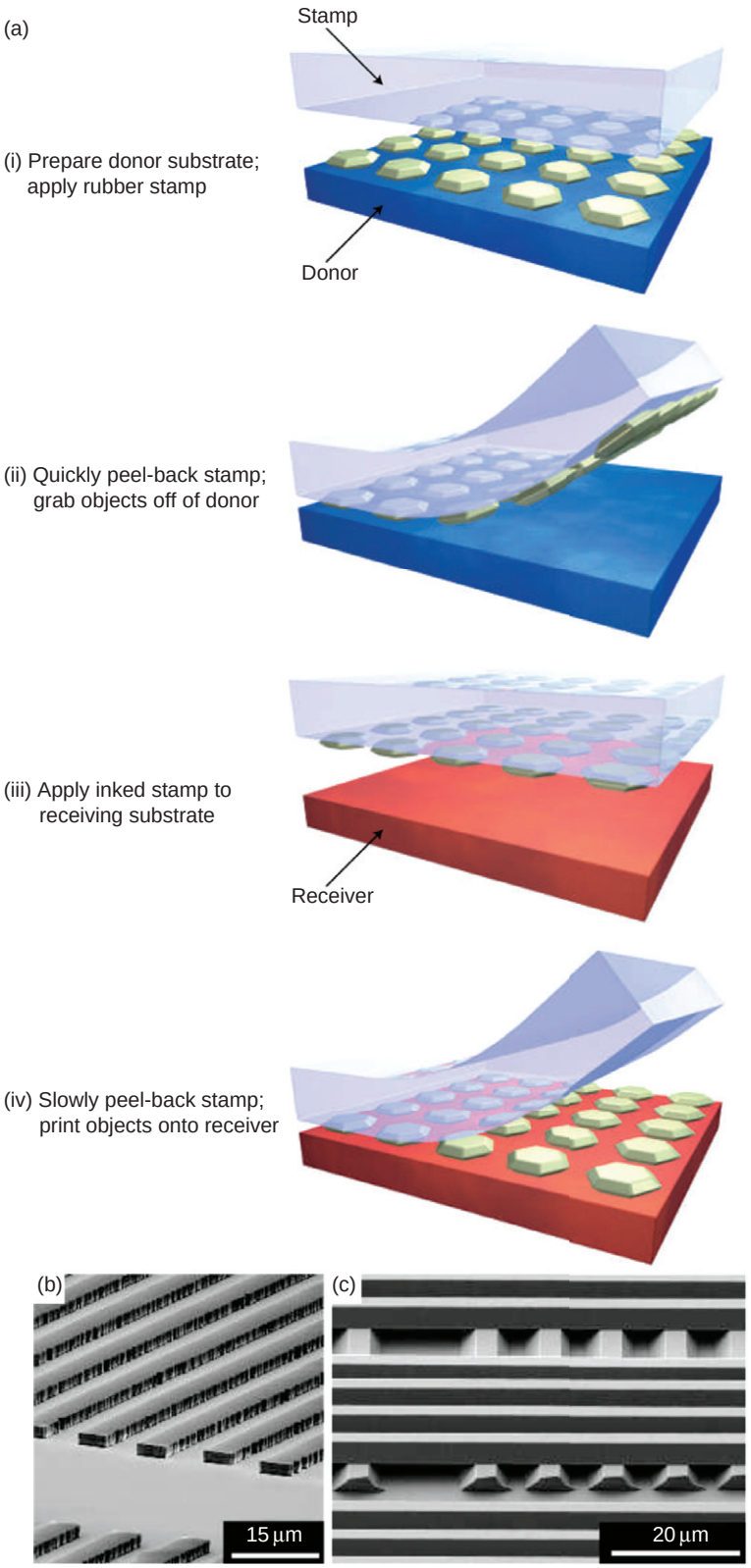

Figure 5 Kinetically controlled decal transfer printing. (a) Schematic drawing of the process used to transfer microfabricated structures from a donor substrate to a polydimethylsiloxane (PDMS) stamp, and then from the PDMS stamp to a receiver substrate. (b and c) scanning electron microscope (SEM) images of two- and three-dimensional structures fabricated by this process. Reproduced with permission from Meitl, M. A.; Zhu, Z. T.; Kumar, V.; *et al. Nat. Mater.* **2006**, *5*, 33–38.[122] Copyright 2006, Nature Publishing Group.

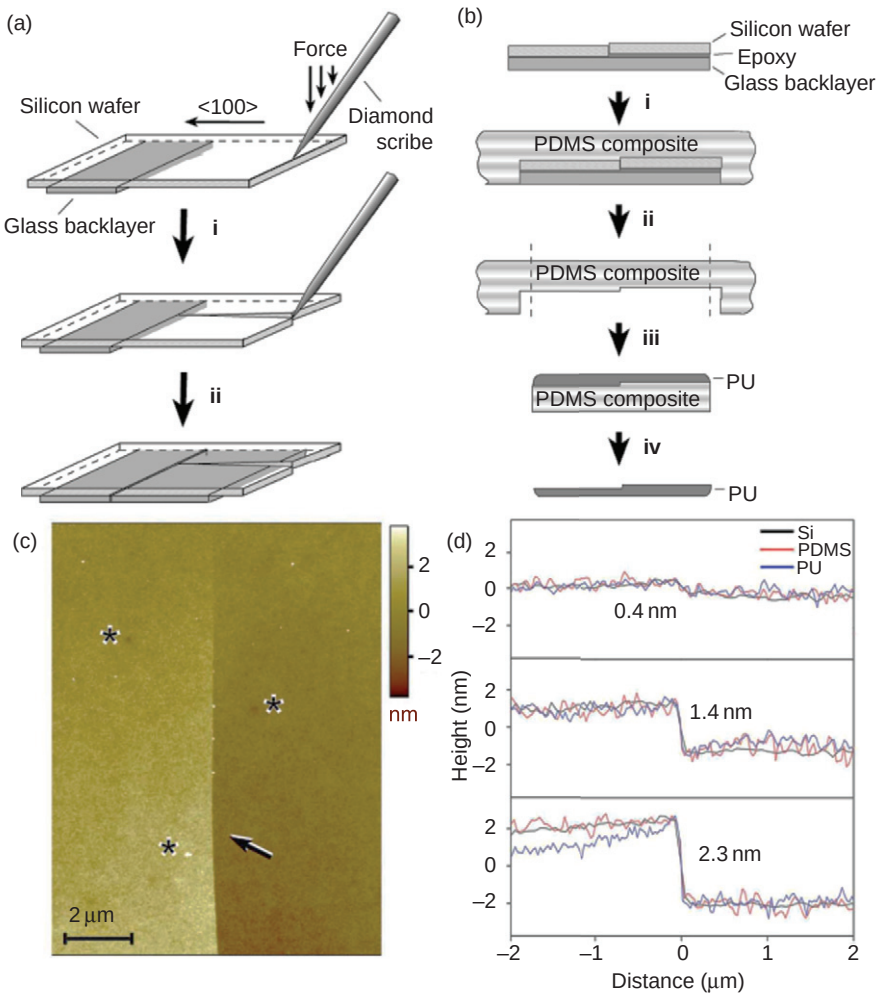

Figure 6 Replication of a 0.4 nm vertical step in polyurethane (PU), mastered from a crack in a silicon substrate, and replicated using a PDMS intermediate. (a) Schematic drawing of the process used to generate a controlled crack in a silicon wafer. (b) Summary of the procedure used to replicate the crack in PU, using a PDMS mold as an intermediate. (c) AFM image of the crack in the PU layer. (d) This replicated step had a minimum measurable height of 0.4 nm. Reproduced with permission from Xu, Q. B.; Mayers, B. T.; Lahav, M.; *et al. J. Am. Chem. Soc.* **2005**, *127*, 854–855.[37] Copyright 2008, American Chemical Society.

of a pattern produced by SFIL. The transparent mold facilitates alignment and registration. SFIL proceeds at ambient temperature, low applied pressures (<10 kPa), and avoids the baking and solvent-processing steps of photolithography. The accuracy of alignment in SFIL is as high as ±10 nm (3σ),[154] and it can produce patterns with 20-nm half-pitch.[152] SFIL thus has potential for incorporation into fabrication of computer memory, and perhaps microprocessors (probably initially in the back plane); it certainly has more than sufficient resolution for use in optical systems.[153] An advantage of SFIL for efficient manufacturing is the ability to produce multiple layers of relief in a resist in a single imprint. This characteristic could reduce the number of steps required to produce vias and other complex structures in three dimensions.

Challenges to overcome for SFIL include deposition of cross-linked resist on the mold (fouling), which can cause irreversible adhesion of the mold to the substrate. Passivation of the surface of the mold using fluorinated silanes can promote release of the mold from the pattern, but fewer than 100 uses per mold is typical.[1] Selectively cleavable cross-linking groups containing acetals enable the mold to be de-fouled by a simple acidic wash.[151,155]

7.11.4.4 Particle Replication in Nonwetting Templates

Over approximately the past 5 years, DeSimone and co-workers have developed a soft lithographic molding procedure called PRINT (**Figure 9**), in which the stamp and substrate are composed of a photochemically cross-linked[116] PFPE.[9,115] This material is a nonwettable and nonswellable elastomer (surface tension ~10 erg cm^{-2}). When molding a material, the low surface energy of the stamp and substrate forces the prepolymer or other material from the space between features, and thus, does not produce a scum layer. Removal of the mold affords unconnected particles, which can be harvested. Williams *et al.*[83] surveyed different PFPEs and determined that PFPE-tetramethacrylate stamps could be molded with the highest resolution of the polymers tested: 20-nm features separated by < 20 nm.

Examples of materials molded using PRINT include poly(ethylene glycol)diacrylate (PEGDA), triacrylate resin,

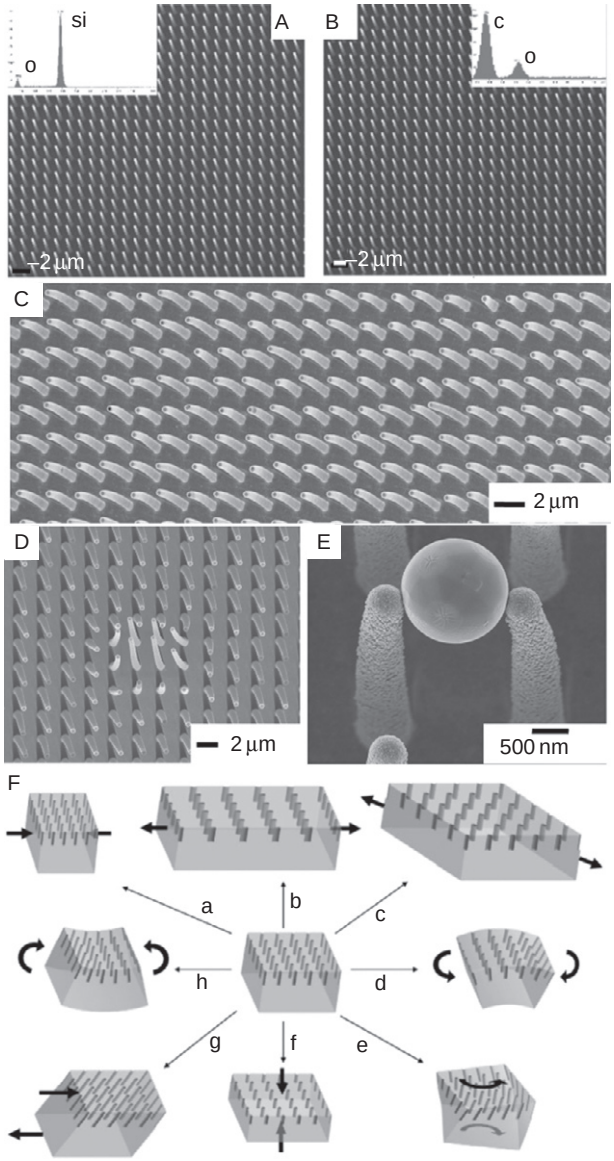

Figure 7 High-aspect ratio epoxy nanoposts obtained using replica molding. (A) SEM image of a silicon master showing the high-aspect-ratio nanoposts. (B) Replica of the silicon master, generated in epoxy, using a PDMS mold as an intermediate. The scale bar is 2 μm. (C) Closer view of epoxy nanoposts. Each nanopost is bowed slightly because it is coated on one side with gold. (D) The posts in the center of the panel are bent because of actuation due to the electron beam. (E) Two nanoposts are grasping a gold nodule ejected from the hearth of the e-beam evaporator. (F) The PDMS mold used to generate the posts can be mechanically deformed during infiltration of the epoxy prepolymer. This action allows skewed and twisted arrays of epoxy nanoposts to be created. (A, B, and F) Reproduced with permission from Pokroy, B.; Epstein, A. K.; Persson-Gulda, M. C. M.; Aizenberg, J. *Adv. Mater.* **2009**, *21*, 463–469.[147] Copyright 2009, Wiley-VCH Verlag GmbH & Co. KGaA.

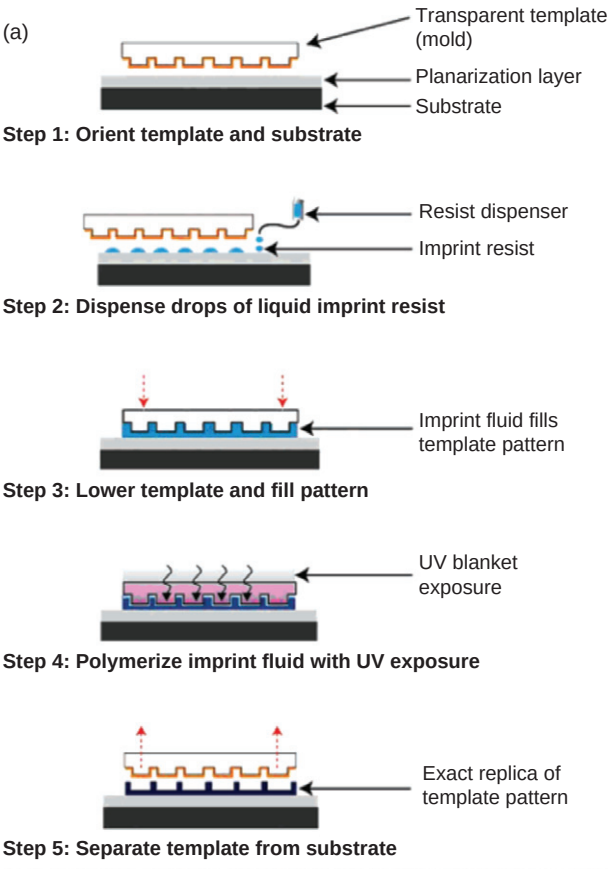

Figure 8 Step-and-flash imprint lithography (SFIL). (a) Schematic summary of the process used. (b) SEM images of structures bearing two layers of relief, but patterned in a single step of SFIL. Reproduced with permission from Heath, W. H.; Palmieri, F.; Adams, J. R.; *et al. Macromolecules* **2008**, *41*, 719–726.[155] Copyright 2008, American Chemical Society.

poly(lactic acid), polypyrrole (PPy),[156] solid particles of proteins,[157] ceramic films from sol–gel precursors, including TiO_2, SnO_2, ZnO, ITO, and $BaTiO_3$,[115] and composite particles,[158] including those incorporating magnetic materials.[159] Figures 9(a)–9(h) show examples of molded particles with different shapes. Particles produced by PRINT are well suited to study the influences of shape and surface functionalization of nanoparticles on the mechanism of uptake by living cells,[11] and are candidates for targeted drug delivery[160] and other biomedical applications.[118] Another possible application is in excitonic solar cells, where the light-absorbing layer requires an interpenetrated heterojunction between electron-donating and electron-accepting materials. The ability to mold films of TiO_2 with post-like nanostructures (30–100 nm in height, with spacing of 30–65 nm), and to infiltrate the spaces between posts with a semiconducting polymer, poly(3-hexylthiophene) (P3HT), produced a photovoltaic device whose power conversion efficiency was double that of a device composed of the

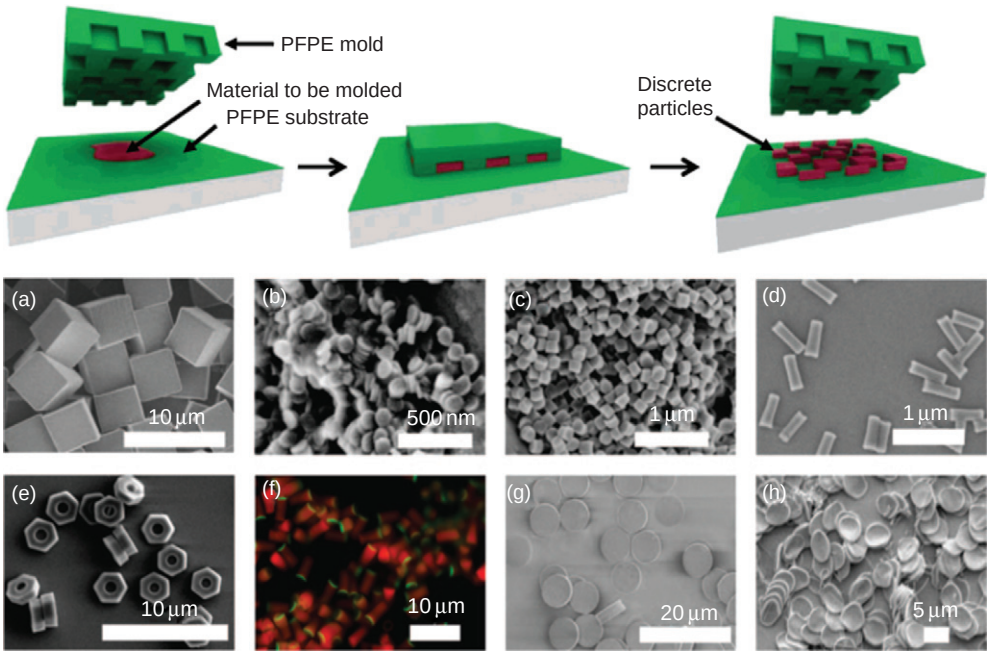

Figure 9 Particle replication in nonwetting templates (PRINT). (Top) Schematic drawing of the process. A perfluoropolyether (PFPE) stamp molds a material (e.g., a liquid prepolymer) against a PFPE substrate. The low surface energy of the stamp and the substrate excludes the prepolymer from entering the space between the stamp and the substrate. Curing the prepolymer and releasing the stamp generates isolated nanoparticles, which can be harvested. Reproduced with permission from Rolland, J. P.; Maynor, B. W.; Euliss, L. E.; *et al. J. Am. Chem. Soc.* **2005**, *127*, 10096–10100.[156] Copyright 2005, American Chemical Society. (a–h) Examples of PRINT particles formed primarily of poly(ethylene oxide) having different shapes and surface functionalities for biological applications. Reproduced with permission from Gratton, S. E. A.; Williams, S. S.; Napier, M. E.; *et al. Acc. Chem. Res.* **2008**, *41*, 1685–1695.[11] Copyright 2008, Wiley-VCH.

same materials, but whose interface between materials was planar.[17] Another potentially useful avenue of research is the development of reel-to-reel processing of particles produced by PRINT.[157]

7.11.4.5 Three-Dimensional Molding

One of the inherent disadvantages of the molding techniques discussed so far is that the patterns produced are essentially 2D. Fabrication and replication of features with significant overhang, or those bearing closed loops, are impossible under normal circumstances without locking the mold to the master irreversibly. The Fourkas laboratory has developed a technique of 3D molding by fabricating 3D master structures using a combination of two techniques: lithography using MPA[72,73,79] and MA-μTM.[78]

MA-μTM is a way of replicating lithographic features bearing tunnels, loops, and interlocking rings. It begins by fabricating a master structure with MPA lithography (**Figure 10(a)**).[78] These masters do not contain closed loops. Instead, loops are filled in by a thin, planar membrane. Curing a PDMS prepolymer over the master and subsequent separation produces a PDMS mold in the form of inverse replica with a void space at the site of the membrane. Gentle compression of the mold causes the opposing faces of the mold at the site of the membrane to form a reversible seal. Infiltrating the mold with a polymer fills the space inside the mold, but is excluded from the site of the membrane. Curing the polymer and releasing it from the mold generate replicas of the masters, but with loops in the replicas at the sites of the membranes in the masters (**Figure 10(b)**). **Figures 10(c)–10(h)** are examples of masters bearing membranes produced by MPA (left-hand side), and replicas produced without the membranes by MA-μTM (right-hand side). Eventually, complex 3D electronic components, such as the gold-coated microinductor fabricated by MPA (**Figures 10(i)** and **10(j)**), could be replicable by soft lithographic molding.[72]

7.11.4.6 Micromolding in Capillaries

MIMIC[143] is a technique that uses the capillarity to fill microfluidic channels with a prepolymer, sol–gel precursor, or other material.[161,162] Two of the advantages of MIMIC are that it automatically places the molded structures onto any substrate onto which the molded material will stick upon hardening, and that it produces isolated features without an interconnecting scum layer. While MIMIC is primarily a technique for microfabrication, it can form structures composed of nanostructured materials, such as inorganic/organic nanocomposites,[163] materials for all-polymer thin-film transistors,[164,165] patterned precipitation of platinum carbonyl clusters,[140] patterning of submicrometer structures (using a commercial DVD as a master) of SiC and SiCN,[166] and patterning microstructures for adhesion of cells.[167] MIMIC can also be combined with physical vapor deposition and nanoskiving to produce parallel nanowire electrodes with a separation of a gap as small as 30 nm and which diverge to form a gap of 30 μm, which is addressable by photolithography with a printed transparency mask.[168]

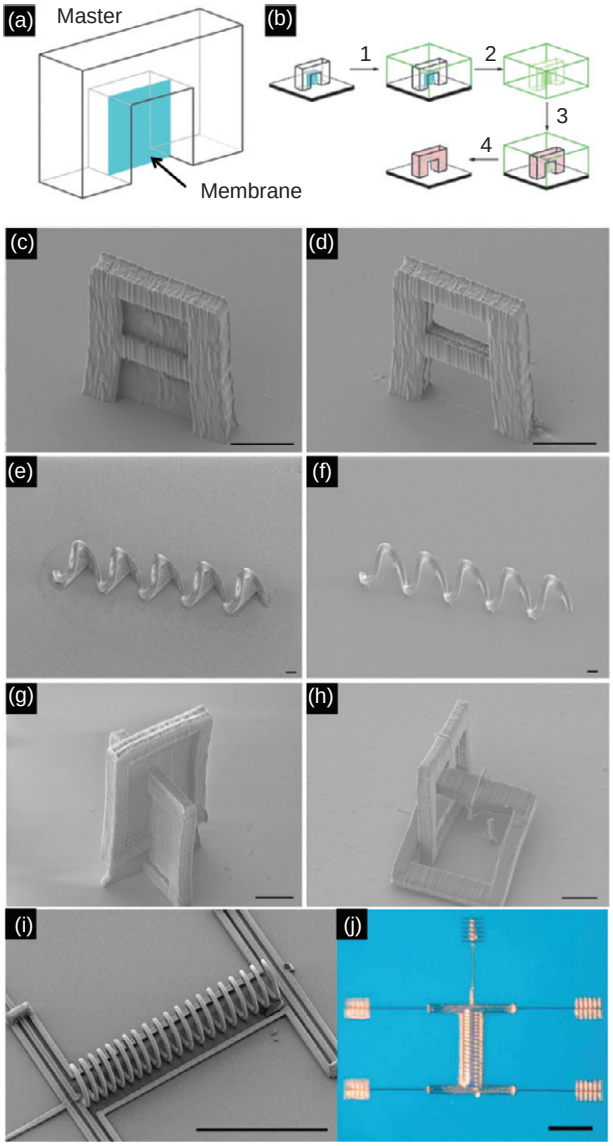

Figure 10 Membrane-assisted fabrication of three-dimensional closed-looped microstructures. (a) Schematic drawing of a master, fabricated using two-photon polymerization, bearing a membrane (blue). A schematic representation of the procedure used to replicate this structure is shown in (b). A PDMS prepolymer is poured over the master and cured (step 1). The PDMS mold is removed. The parts of the mold on either side of the region defined by the membrane form a reversible seal (step 2). Infiltration of a prepolymer fills the mold, except for the region defined by the membrane in the master (step 3). Curing the infiltrated polymer, and releasing the mold, produces an arch without a membrane (step 4). Images of three-dimensional master structures bearing membranes closing the loops (c, e, and g) and the replicas (d, f, and h) without the loops. The scale bars are 10 μm. Reproduced with permission from LaFratta, C. N.; Li, L. J.; Fourkas, J. T. *Proc. Natl. Acad. Sci. U.S.A.* **2006**, *103*, 8589–8594.[78] Copyright 2006, National Academy of Sciences U.S.A. SEM (i) and optical (j) images of three-dimensional microinductors. The scale bars are 100 μm. Reproduced with permission from LaFratta, C. N.; Fourkas, J. T.; Baldacchini, T.; Farrer, R. A. *Angew. Chem., Int. Ed.* **2007**, *46*, 6238–6258.[79] Copyright 2007, Wiley-VCH Verlag GmbH & Co. KGaA.

7.11.4.7 Solvent-Assisted Micromolding

SAMIM is an embossing technique in which a solvent softens a polymer in a form in which it can be molded by a stamp (usually PDMS). As the solvent evaporates, the polymer conforms to the features of the PDMS mold. SAMIM has produced features in novolac photoresist with linewidths of 60 nm.[144] This process is also amenable to several other polymers, including PS,[144] PMMA,[144] and cellulose acetate (CA).[144] Replication of nanoscale features in some materials requires a polymer with a higher modulus than that of PDMS. Lee *et al.*[106] used stamp composed of Norland Optical Adhesive 63 (NOA63) and PEGDA to emboss 160 nm features in a film of poly(4-vinylpyridine). In other examples, Huang *et al.*[169] used CO_2 gas as a plasticizer to emboss an array of polymeric microlenses, and Mazzoldi *et al.*[170] used PDMS stamps to mold a dispersion of carbon nanotubes in a matrix of poly(vinyl alcohol) and poly(vinyl amine) for actuation. One of the disadvantages of SAMIM is the extent to which uptake of the solvent by the stamp swells and distorts the pattern. See Lee *et al.*[171] for a discussion of PDMS stamps to different solvents. Like most forms of molding, but unlike MIMIC and PRINT, SAMIM leaves behind a scum layer in the patterned polymer film.

7.11.5 2D and 3D Fabrication using Optical Soft Lithography

7.11.5.1 Introduction

One-to-one transfer of patterns by physical contact – for example, printing and molding – is not the only way to extract nanoscale information from patterned elastomeric stamps. Exposure of a photoresist through a topographically patterned, conformal phase mask can produce nanopatterns by two related mechanisms. The first is phase-shifting edge lithography, where a PDMS stamp, placed into contact with a photoresist film, produces lines around the perimeters of the relief features where the intensity of the light drops to zero.[1] The second is proximity-field nanopatterning (PnP), developed by Rogers and co-workers, where a stamp molds the surface of a several-micrometer-thick photoresist film; subsequent irradiation produces a 3D interference pattern, which exposes the volume of the photoresist in the regions of maximum constructive interference, and generates complex 3D periodic or aperiodic structures.[172,173]

7.11.5.2 3D Fabrication by Phase-Shifting Edge Lithography

Elastomeric stamps produced by soft lithographic techniques[67] can be used as phase masks for near-field, contact-mode photolithography.[1] The technique relies on the phenomenon of significant reduction in intensity of light around the perimeters of relief structures on a phase mask in contact with a substrate bearing a film of photoresist. Irradiation of the mask in contact with the substrate produces lines in positive photoresist and trenches in negative photoresist that can be significantly thinner than the broadband, incoherent light source used for irradiation. Resolution of 50 nm has been demonstrated.[174,175] For a detailed quantitative description of the mechanism of the process, see the work by Li *et al.*,[30] Rogers *et al.*,[33] and Paul *et al.*[173]

Patterns in photoresist produced by this simple and inexpensive technique can be transferred to the substrate using RIE or to thin films using typical liftoff procedures. To date, the patterns formed by phase-shifting edge lithography have been used to fabricate several structures: single-crystalline nanowires of Si,[176] gold, and silica nanowires on planar[33] and nonplanar substrates,[32] aperture elements for mid-infrared frequency-selective

surfaces,[177] and single-crystalline nanowires of silicon.[176] In combination with etching, physical vapor deposition, and liftoff, phase-shifting photolithography has been employed by Odom and co-workers for the fabrication of mesoscale pyramids with plasmonic properties,[178,179] or combined with controlled undercutting to produce other periodic arrays of structures.[103]

7.11.5.3 3D Fabrication by Proximity-Field Nanopatterning

An extension of phase-shifting edge lithography, called PnP, produces periodic 3D structures in embossed films of photoresist.[134,180] The procedure is conceptually similar to that described by Paul *et al.*,[173] in which embossed, thick films of photoresist were used as a phase mask for the exposure of the resist below. This process produced contoured features with sizes as small as 70 nm.[173] Figure 11 summarizes an extension of this concept to produce complex 3D structures. First, a stamp embosses the surface of a photoresist film (Figures 11(a) and 11(b)). This embossed pattern of photoresist becomes the phase-shifting mask for its own exposure. Irradiation produces a complex 3D interference pattern that exposes the photoresist to two-photon absorption in the regions of greatest constructive interference.[172] Washing out the unexposed polymer (for negative-tone photoresists, often SU8) produces a complex, but calculable, 3D pattern, in films that can be as thick as 20 μm. These polymer–air structures can serve as 3D photonic crystals.[181] Infiltration of these porous structures with a prepolymer, and concurrent imaging and writing with a multiphoton confocal microscope, can incorporate site-specific defects into these structures.[182] Chemical vapor deposition can fill the void space with silicon. Subsequent oxidative degradation of the polymer produces silicon–air structures.[181] Embossing the photoresist with a fivefold Penrose quasicrystalline pattern produces 3D structures with quasicrystalline symmetry in the plane parallel to the embossed surface of the film, and aperiodicity in the plane perpendicular to the surface of the film.[183] A similar procedure of embossing and exposure can directly pattern 3D, inorganic structures in photoresists based on spin-on glass.[184]

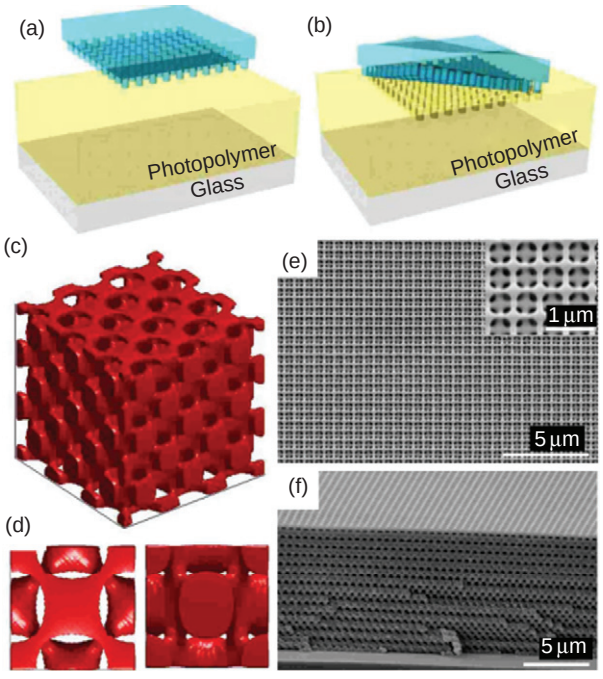

Figure 11 Proximity-field nanopatterning of three-dimensional structures. (a and b) Schematic drawing of the procedure used to emboss a film of photopolymer with an elastomeric mask bearing relief structures. The embossed film serves as its own phase mask. The pattern of constructive and destructive interference within the photopolymer film produces a three-dimensional structure modeled in (c) and (d), and shown in the SEM images in (e) and (f). Reproduced with permission from Shir, D.; Nelson, E. C.; Chen, Y. C.; *et al. Appl. Phys. Lett.* **2009**, *94*, 011101.[181] Copyright 2009, American Institute of Physics.

7.11.6 Nanoskiving

7.11.6.1 Introduction

Nanoskiving is a simple and inexpensive method of nanofabrication based on mechanical sectioning of thin films. The process comprises three steps: (1) deposition of a metallic, semiconducting, ceramic, or polymeric thin film onto an epoxy substrate (which may be topographically patterned by soft lithography); (2) embedding this substrate in epoxy, to form an epoxy block, with the film as an inclusion; and, the key step, (3) sectioning the epoxy block into slabs with an ultramicrotome. These epoxy slabs (30 nm–10 μm thick) contain nanostructures whose lateral dimensions are determined by the thicknesses of the embedded thin films (10 nm linewidths demonstrated). The structures produced by nanoskiving would be difficult or impossible to produce using other procedures, and these structures can be transferred easily to almost any substrate.[66]

Nanoskiving forms intact structures from films of relatively soft and compliant metals (softer than platinum, or those with bulk values of hardness < 500 MPa, Vickers scale), while hard and stiff materials tend to fragment (those harder than nickel, or > 500 MPa). The Whitesides laboratory has successfully formed nanostructures of aluminum, copper, silver, gold, lead, bismuth, palladium, platinum, nickel, germanium, silicon dioxide, all conducting and semiconducting polymers tested, and films of lead sulfide nanocrystals.[185]

7.11.6.2 Sectioning Planar Thin Films

Stacking spin-coated films of conjugated polymers and nanoskiving permit one to obtain nanowires singly, in bundles, or in parallel with high pitch.[186] The nanowires produced using this method had rectangular cross sections. In one variant of this procedure, spin-coating two conjugated polymers, poly(benizimidazo benzophenantrholine) ladder (BBL) and poly(2-methoxy-5-(2′-ethylhexyloxy)-1,4-phenylenevinylene) (MEH-PPV) alternately on the same substrate, produced a laminated film in which fifty 100-nm layers of BBL were separated by fifty 100-nm layers of MEH-PPV. Sectioning this 10-μm-thick film provided cross sections that bore 100-nm-wide strips of the two conjugated polymers. Etching the MEH-PPV with an air plasma left behind parallel BBL nanowires (Figures 12(a) and 12(b)), and dissolving BBL with methanesulfonic acid left behind MEH-PPV nanowires (Figures 12(c) and 12(d)). Figure 12(e) is a plot of current

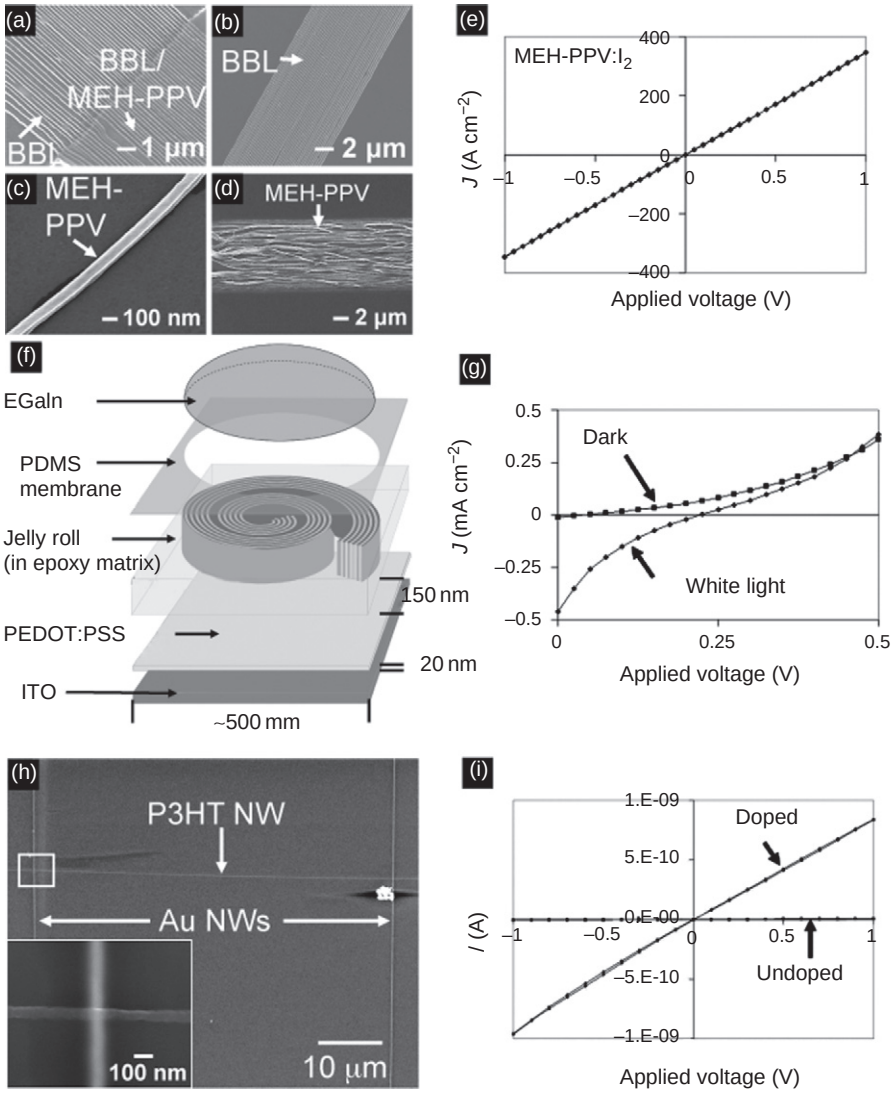

Figure 12 Nanowires and heterostructures of conjugated polymers formed by nanoskiving and electrical characteristics of the structures. (a–d) Conjugated polymer nanowires and (e) plot of current density vs. voltage of a group of MEH-PPV nanowires, doped by iodine vapor, shown in (d). Reproduced with permission from Lipomi, D. J.; Chiechi, R. C.; Dickey, M. D.; Whitesides, G. M. *Nano Lett.* **2008**, *8*, 2100–2105.[186] Copyright 2008, American Chemical Society. (f) A P3HT nanowire spanning the gap between two gold nanowire electrodes, and (g) a plot of current density vs. voltage of the nanowire, doped by iodine. Reproduced with permission from Lipomi, D. J.; Ilievski, F.; Wiley, B. J.; *et al. ACS Nano* **2009**, *3*, 3315–3325.[187] Copyright 2009, American Chemical Society. (h) Schematic drawing of an ordered bulk heterjunction of conjugated polymers (a jelly roll). (i) When placed between electrodes, the jelly roll produces a photovoltaic effect. Reproduced with permission from Lipomi, D. J.; Chiechi, R. C.; Reus, W. F.; Whitesides, G. M. *Adv. Funct. Mater.* **2008**, *18*, 3469–3477.[44] Copyright 2008, Wiley-VCH Verlag GmbH & Co. KGaA.

density versus voltage (J–V) of a group of MEH-PPV nanowires, of the type shown in Figure 12(d), when exposed to I_2 vapor.

A similar procedure of fabrication, in which a material of interest is stacked with a sacrificial material, can be used to form parallel nanowires of gold[35] or palladium.[187] Sectioning photolithographically patterned strips of gold into collinear nanowires of gold can produce nanoelectrodes for electrochemistry,[35] as well as monodisperse plasmon resonators.[188] Wiley *et al.*[14] showed that sectioning single-crystalline gold microplates produced single-crystalline gold nanowires. These nanowires were of sufficient quality to support surface plasmon polaritons, which could be used to confine light to subwavelength lateral dimensions for nanophotonic applications. Lipomi *et al.* were also able to stack, roll, and cut sub-100-nm layers of conjugated polymers of MEH-PPV and BBL to produce heterostructures of conjugated polymers with high interfacial surface area. When placed between electrodes and irradiated with white light (which excites both polymers) or red light (which excites only BBL), these heterostructures produced a photovoltaic effect due to photoinduced charge transfer within the slab (Figures 12(f) and 12(g)).[44]

It was also possible to position structures produced by nanowires using noncontact manipulation with magnetic interactions. To form electrically continuous junctions between nanowires of different types, two parallel gold nanowires, embedded in the same epoxy slab, were deposited on an insulating substrate. Separately, a film of P3HT with nickel nanopowder was embedded and sectioned into 100-nm-thick

slabs containing P3HT nanowires and nickel powder. Floating such a slab onto a pool of water over the predeposited parallel gold nanowires, positioning it with an external permanent magnet, and allowing the water to evaporate, produced an electrically contiguous geometry of nanowires in which the P3HT nanowire spanned the 50-μm gap between gold nanowires (Figure 12(h)). This geometry could be useful in measuring nanoscale charge transport in optoelectronic polymers, and in the fabrication of chemical sensors[189,190] or field-effect transistors based on single nanowires.[191] P3HT undergoes an insulator-to-metal transition upon exposure to I_2.[192] Figure 12(i) is an *I*–*V* plot of the nanowire when exposed to I_2 ('doped') and in the absence of the I_2 ('undoped'). It should also be possible to use this technique for four-terminal measurements, which would allow decoupling of the contact resistance from the true resistance of a nanowire.[189]

7.11.6.3 Sectioning Parallel to Arrays of Nanoposts

Applications such as optical filters,[52,193] substrates for surface-enhanced Raman spectroscopy,[194,195] and metamaterials[43,196–198] required 2D arrays of nanostructures. Using a procedure that combined molding an epoxy substrate by soft lithography, thin-film deposition, embedding, and sectioning parallel to the plane of topography, 2D arrays of nanostructures could be produced using nanoskiving. [199] Figure 13 shows an example of this process. First, an array of epoxy nanoposts was molded by soft lithography. This array was coated conformally with gold by sputter coating, then coated by PPy using electrochemical growth, then coated a second time with gold. These procedures produced an array of four-layered, coaxial nanoposts with radial symmetry.[199] When embedded in epoxy and sectioned into slabs, the slabs contained radially symmetric discs of epoxy, gold, PPy, and gold. These arrays could be transferred to essentially any substrate. An optional step was to etch the organic components using an air plasma. Etching left behind arrays of free-standing, concentric rings of gold. Figure 14 shows a series of structures fabricated by this and related procedures.[199]

There are at least five important aspects of the structures produced that cannot be replicated easily, if at all, with other techniques: (1) the linewidths of the structures are determined by the thickness of the thin film, not the dimensions of the original topographic master; (2) the height of the structures can be tuned over a large range (80 nm–2 μm demonstrated in Figure 14), simply by changing the set thickness on the ultramicrotome; (3) the structures can be composed of two or more materials in the same plane, without the need for multiple steps of patterning; (4) the components can be in physical contact in the lateral dimension; and (5) many slabs may be obtained from a single embedded structure (we have produced as many as 60 consecutive cross sections, 100 nm thick, from a single embedded array of 8-μm, gold-coated epoxy nanoposts).[199]

7.11.6.4 Placement of Arrays on Arbitrary Substrates

The thin slab of epoxy in which the structures produced by nanoskiving are embedded provides a visible handle to transfer arrays to substrates.[34] There is, thus, a major challenge in

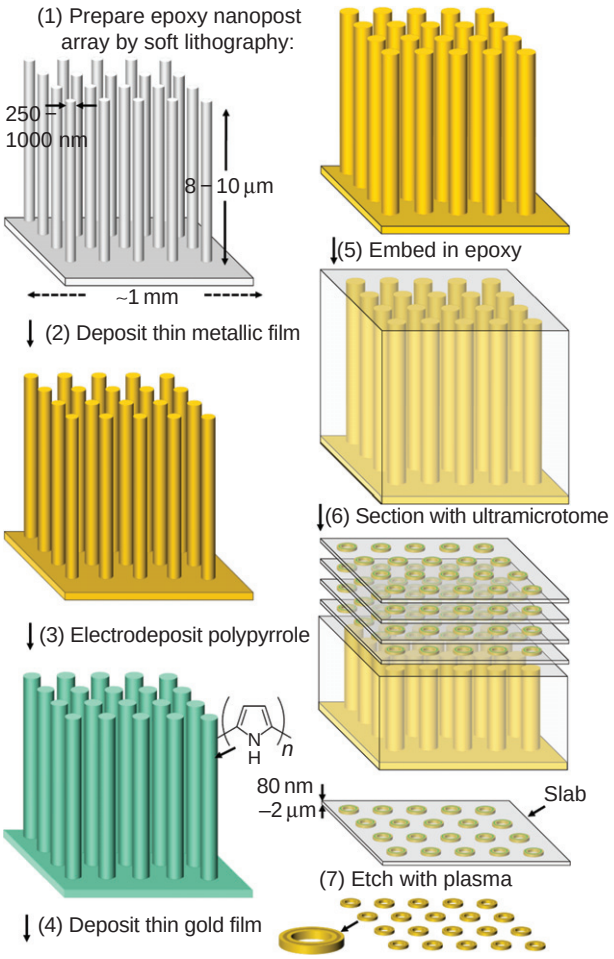

Figure 13 Summary of an example of the process used to fabricate two- and three-dimensional nanostructures by growing radially symmetric nanoposts of multiple materials. Replica molding produces an array of epoxy nanoposts (1). Sputter-deposition coats the array conformally with a thin film of gold (2). Electrodeposition of polypyrrole, using the gold as a working electrode, produces a conformal film of the conductive polymer (3). A second sputter deposition of gold produces radially symmetric, three-component nanoposts (4). Embedding the array produces a block (5), which is sectioned by the microtome into slabs (6). Plasma etching produces an array of free-standing, concentric gold rings separated by a gap whose size is determined by the electrodeposition of polypyrrole (7). Reproduced with permission from Lipomi, D. J.; Kats, M. A.; Kim, P.; *et al. ACS Nano* **2010**, *4*, 4017–4026.[199] Copyright 2010, American Chemical Society.

optics to which nanoskiving seems particularly (perhaps uniquely) well suited – modifying the cleaved facets of optical fibers with arrays of nanostructures. The ability to control the emission from fibers using filters or polarizers, and the fabrication of sensors for *in situ*, label-free detection of chemical or biological analytes using either surface-enhanced Raman scattering (SERS)[200] or localized surface plasmon resonances (LSPRs),[201] are possible applications of modified optical fibers.[202] Attachment of plasmonic arrays to the cleaved facets of fibers is not straightforward by conventional means, however. Photolithographic patterning of the facets of fibers would require deposition, exposure, and

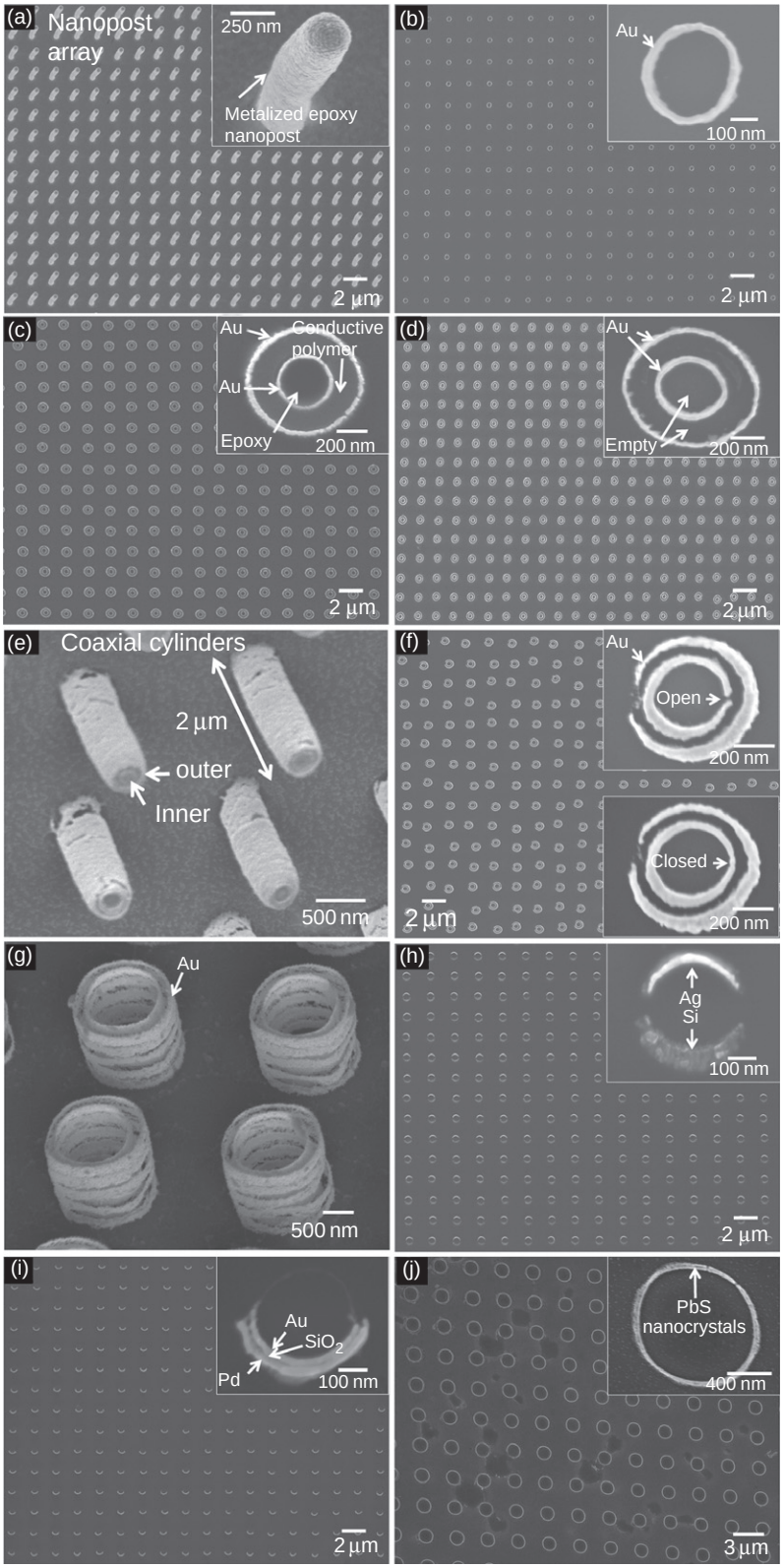

Figure 14 Scanning electron microscope (SEM) images of metallic, polymeric, and semiconducting nanostructures produced by nanoskiving. (a) Coaxial nanoposts composed of a core of epoxy, and layers of gold, polypyrrole, and gold. (b) An array of single rings of gold. (c) An array of discs obtained by sectioning the nanoposts shown in (a). (d) An array of concentric rings of gold obtained by removing the organic components of the structures shown in (c) using an air plasma. (e) High-aspect-ratio concentric cylinders of gold. (f) Counterfacing, concentric split rings of gold. (g) Coaxial stacked rings obtained from a master with corrugated sidewalls. (h) Counterfacing crescents of silver and silicon. (i) Three-layer crescents comprising an inner shell of gold and an outer shell of palladium. These layers are separated by a thin layer of silicon dioxide.(j) An array of rings of lead sulfide (PbS) nanocrystals. Reproduced with permission from Lipomi, D. J.; Kats, M. A.; Kim, P.; *et al. ACS Nano* **2010**, *4*, 4017–4026.[199] Copyright 2010, American Chemical Society.

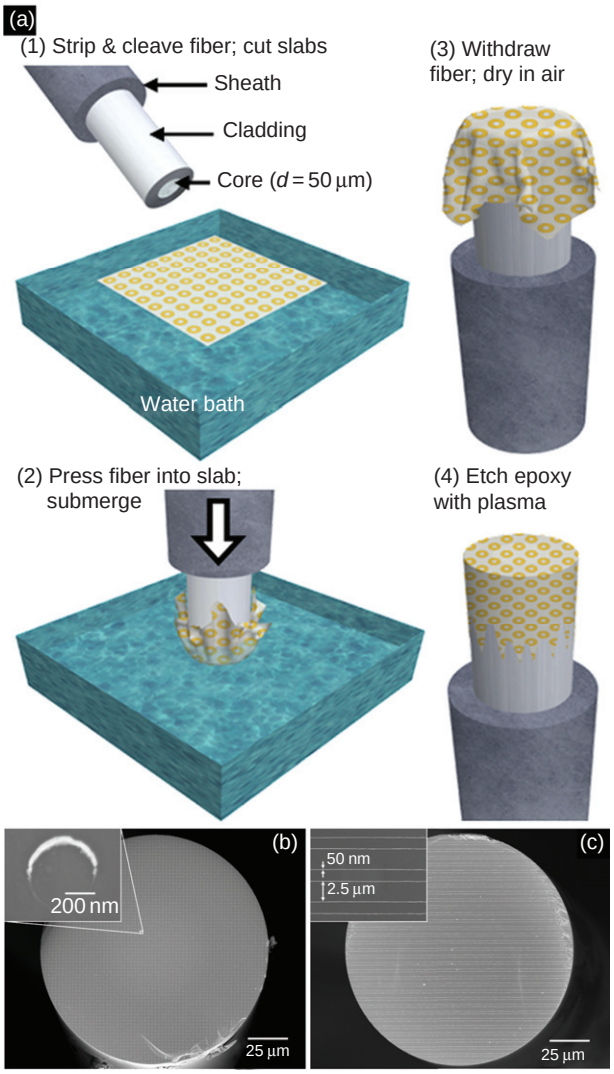

Figure 15 Transfer of arrays of nanoparticles to the cleaved facets of optical fibers. (a) Schematic drawing of the procedure used to capture floating slabs by submerging them with an optical fiber using a perpendicular trajectory. (b) The facet of an optical fiber bearing an array of gold crescents like the one shown in the inset. (c) Another facet, bearing a grating of gold nanowires with widths of 50 nm. Reproduced with permission from Lipomi, D. J.; Martinez, R. V.; Kats, M. A.; *et al. Nano Lett.*, **2011**, online.[205] Copyright 2010, American Chemical Society.

development of photoresist on a small area ($d \sim 100\,\mu m$).[102] Examples of unconventional methods to integrate plasmonic elements with optical fibers include anisotropic chemical etching, to form arrays of sharp cones,[203] and transferring gold structures fabricated by EBL from a surface to which gold adhered weakly.[204]

Figure 15 summarizes a method to mount arrays of metallic nanostructures on the facets of optical fibers.[205] Pressing down on a floating slab with the tip of an optical fiber submerges the slab, which wraps itself around the tip of the fiber upon withdrawal from the water-filled trough of the ultramicrotome. After allowing the water on the tip of the fiber to evaporate, exposure to an air plasma using a benchtop plasma cleaner etches the epoxy matrix and leaves behind the nanostructures only on the facet of the fiber (Figures 15(b) and 15(c)).[205]

7.11.7 Conclusions

Soft lithography comprises a group of methods of micro- and nanofabrication and has distinct advantages and limitations. Common to all soft lithographic approaches to nanofabrication are their low cost and simplicity, and applicability to soft materials and unusual form factors. Soft lithography is distinct from conventional forms of fabrication in that it is based on physical contact and its resolution is, in principle, limited by the van der Waals radius. In reality, the sizes of the smallest features obtainable are dictated by a variety of factors. The elasticity of the stamp, which affords it the ability to conform to nonplanar or compliant substrates, also has the effect of inducing long-range distortions in the patterns that are transferred. The significance of these distortions depends on the application.

Soft lithographic printing and molding are like photolithography, in that they do not generate nanoscale information *de novo*. Rather, stamps and molds replicate patterns created by topographic templates, which are usually created using conventional lithography. Stamps and molds in soft lithography, thus, play the roles masks in photolithography. The exceptions are phase-shifting optical lithography and nanoskiving, where the lateral features of the transferred patterns are determined by the nulls in optical intensity around the perimeters of relief features and the thicknesses of deposited thin films, respectively. For these 'edge lithographic' techniques, nanoscale information is generated *de novo* during the process of replication, and thus they can be treated as techniques for simultaneous mastering and replication.

Soft lithography already represents a convenient set of approaches to problems in a wide range of disciplines in the research community. Areas of research in which we believe soft lithography could play a significant role include printed organic electronics, nanostructures for plasmonics and optics, patterned surfaces for cell biology, nanofluidics, nanoelectromechanical systems, and studies of single molecules. The applications of nanotechnology enabled by soft lithography closest to commercialization will probably be those that reduce the costs of existing devices. These applications include inexpensive sub-100-nm fabrication for microelectronics by SFIL[56] or by μCP of monolayer resists.[25] Some of the most important applications found for any new technology have been, however, impossible to predict. The best possible outcomes of research in soft lithography – or any tool for unconventional nanofabrication – are to increase the accessibility of nanoscience in the research laboratory, to reduce the cost of commercial production, to realize theorized applications of nanoscience, and to discover unforeseen ones.

Acknowledgments

This research was supported by the National Science Foundation under award PHY-0646094.

References

1. Gates, B. D.; Xu, Q. B.; Stewart, M.; *et al. Chem. Rev.* **2005**, *105*, 1171–1196.
2. Willson, C. G.; Roman, B. J. *ACS Nano* **2008**, *2*, 1323–1328.
3. Menard, E.; Meitl, M. A.; Sun, Y. G.; *et al. Chem. Rev.* **2007**, *107*, 1117–1160.
4. Kim, D. H.; Rogers, J. A. *Adv. Mater.* **2008**, *20*, 4887–4892.
5. Whitesides, G. M.; Lipomi, D. J. *Faraday Disc.* **2009**, *143*, 373–384.
6. Yun, M. H.; Myung, N. V.; Vasquez, R. P.; *et al. Nano Lett.* **2004**, *4*, 419–422.
7. Cui, Y.; Wei, Q. Q.; Park, H. K.; Lieber, C. M. *Science* **2001**, *293*, 1289–1292.
8. Ramanathan, K.; Bangar, M. A.; Yun, M.; *et al. J. Am. Chem. Soc.* **2005**, *127*, 496–497.
9. Whitesides, G. M.; Ostuni, E.; Takayama, S.; *et al. Annu. Rev. Biomed. Eng.* **2001**, *3*, 335–373.
10. Hong, J.; Edel, J. B.; deMello, A. J. *Drug Discov. Today* **2009**, *14*, 134–146.
11. Gratton, S. E. A.; Williams, S. S.; Napier, M. E.; *et al. Acc. Chem. Res.* **2008**, *41*, 1685–1695.
12. Arakawa, H.; Aresta, M.; Armor, J. N.; *et al. Chem. Rev.* **2001**, *101*, 953–996.
13. Stewart, M. E.; Anderton, C. R.; Thompson, L. B.; *et al. Chem. Rev.* **2008**, *108*, 494–521.
14. Wiley, B. J.; Lipomi, D. I.; Bao, J. M.; *et al. Nano Lett.* **2008**, *8*, 3023–3028.
15. Xu, Q. B.; Bao, J. M.; Rioux, R. M.; *et al. Nano Lett.* **2007**, *7*, 2800–2805.
16. Boettcher, S. W.; Spurgeon, J. M.; Putnam, M. C.; *et al. Science* **2010**, *327*, 185–187.
17. Williams, S. S.; Hampton, M. J.; Gowrishankar, V.; *et al. Chem. Mater.* **2008**, *20*, 5229–5234.
18. Garcia-Martinez, J. *Nanotechnology for the Energy Challenge*; Wiley-VCH, Weinheim, 2010.
19. Martinez, A. W.; Phillips, S. T.; Butte, M. J.; Whitesides, G. M. *Angew. Chem., Int. Ed.* **2007**, *46*, 1318–1320.
20. Love, J. C.; Estroff, L. A.; Kriebel, J. K.; *et al. Chem. Rev.* **2005**, *105*, 1103–1169.
21. Aizenberg, J.; Black, A. J.; Whitesides, G. M. *Nature* **1999**, *398*, 495–498.
22. Hawker, C. J.; Russell, T. P. *MRS Bull.* **2005**, *30*, 952–966.
23. Xia, Y. N.; Whitesides, G. M. *Angew. Chem., Int. Ed.* **1998**, *37*, 551–575.
24. Qin, D.; Xia, Y. N.; Whitesides, G. M. *Nat. Protoc.* **2010**, *5*, 491–502.
25. Biebuyck, H. A.; Larsen, N. B.; Delamarche, E.; Michel, B. *IBM J. Res. Dev.* **1997**, *41*, 159–170.
26. Xia, Y. N.; Qin, D.; Whitesides, G. M. *Adv. Mater.* **1996**, *8*, 1015–1017.
27. Xia, Y. N.; Whitesides, G. M. *Langmuir* **1997**, *13*, 2059–2067.
28. Xia, Y. N.; Kim, E.; Zhao, X. M.; *et al. Science* **1996**, *273*, 347–349.
29. Xia, Y. N.; McClelland, J. J.; Gupta, R.; *et al. Adv. Mater.* **1997**, *9*, 147–149.
30. Li, Z. Y.; Yin, Y. D.; Xia, Y. N. *Appl. Phys. Lett.* **2001**, *78*, 2431–2433.
31. Maria, J.; Jeon, S.; Rogers, J. A. *J. Photochem. Photobiol., A* **2004**, *166*, 149–154.
32. Rogers, J. A.; Paul, K. E.; Jackman, R. J.; Whitesides, G. M. *Appl. Phys. Lett.* **1997**, *70*, 2658–2660.
33. Rogers, J. A.; Paul, K. E.; Jackman, R. J.; Whitesides, G. M. *J. Vac. Sci. Technol., A* **1998**, *16*, 59–68.
34. Xu, Q.; Rioux, R. M.; Whitesides, G. M. *ACS Nano* **2007**, *1*, 215–227.
35. Xu, Q. B.; Gates, B. D.; Whitesides, G. M. *J. Am. Chem. Soc.* **2004**, *126*, 1332–1333.
36. Xia, Y. N.; Rogers, J. A.; Paul, K. E.; Whitesides, G. M. *Chem. Rev.* **1999**, *99*, 1823–1848.
37. Xu, Q. B.; Mayers, B. T.; Lahav, M.; *et al. J. Am. Chem. Soc.* **2005**, *127*, 854–855.
38. Favier, F.; Walter, E. C.; Zach, M. P.; *et al. Science* **2001**, *293*, 2227–2231.
39. Li, Q. G.; Olson, J. B.; Penner, R. M. *Chem. Mater.* **2004**, *16*, 3402–3405.
40. Walter, E. C.; Murray, B. J.; Favier, F.; *et al. J. Phys. Chem. B* **2002**, *106*, 11407–11411.
41. Zach, M. P.; Newberg, J. T.; Sierra, L.; *et al. J. Phys. Chem. B* **2003**, *107*, 5393–5397.
42. Zach, M. P.; Ng, K. H.; Penner, R. M. *Science* **2000**, *290*, 2120–2123.
43. Gwinner, M. C.; Koroknay, E.; Fu, L. W.; *et al. Small* **2009**, *5*, 400–406.
44. Lipomi, D. J.; Chiechi, R. C.; Reus, W. F.; Whitesides, G. M. *Adv. Funct. Mater.* **2008**, *18*, 3469–3477.
45. Melosh, N. A.; Boukai, A.; Diana, F.; *et al. Science* **2003**, *300*, 112–115.
46. Kostovski, G.; Mitchell, A.; Holland, A.; Austin, M. *Appl. Phys. Lett.* **2008**, *92*, 223109-1–223109-3.
47. Tang, J. Y.; Wang, Y. L.; Klare, J. E.; *et al. Angew. Chem., Int. Ed.* **2007**, *46*, 3892–3895.
48. Gates, B. D.; Xu, Q. B.; Thalladi, V. R.; *et al. Angew. Chem., Int. Ed.* **2004**, *43*, 2780–2783.
49. Natelson, D.; Willett, R. L.; West, K. W.; Pfeiffer, L. N. *Appl. Phys. Lett.* **2000**, *77*, 1991–1993.
50. Stormer, H. L.; Baldwin, K. W.; Pfeiffer, L. N.; West, K. W. *Appl. Phys. Lett.* **1991**, *59*, 1111–1113.
51. Pfeiffer, L.; West, K. W.; Stormer, H. L.; *et al. J. Appl. Phys. Lett.* **1990**, *56*, 1697–1699.
52. Love, J. C.; Paul, K. E.; Whitesides, G. M. *Adv. Mater.* **2001**, *13*, 604–607.
53. Aizenberg, J.; Black, A. J.; Whitesides, G. M. *Nature* **1998**, *394*, 868–871.
54. Black, A. J.; Paul, K. E.; Aizenberg, J.; Whitesides, G. M. *J. Am. Chem. Soc.* **1999**, *121*, 8356–8365.
55. Sundar, V. C.; Aizenberg, J. *Appl. Phys. Lett.* **2003**, *83*, 2259–2261.
56. Willson, C. G. *J. Photopolym. Sci. Technol.* **2009**, *22*, 147–153.
57. Weibel, D. B.; DiLuzio, W. R.; Whitesides, G. M. *Nat. Rev. Microbiol.* **2007**, *5*, 209–218.
58. Goh, C.; Coakley, K. M.; McGehee, M. D. *Nano Lett.* **2005**, *5*, 1545–1549.
59. Whitesides, G. M. *Nature* **2006**, *442*, 368–373.
60. Baret, J. C.; Miller, O. J.; Taly, V.; *et al. Lab Chip* **2009**, *9*, 1850–1858.
61. Metzker, M. L. *Nat. Rev. Genet.* **2010**, *11*, 31–46.
62. Tewhey, R.; Warner, J. B.; Nakano, M.; *et al. Nat. Biotechnol.* **2009**, *27*, 1025–1031.
63. Piner, R. D.; Zhu, J.; Xu, F.; *et al. Science* **1999**, *283*, 661–663.
64. Salaita, K.; Wang, Y. H.; Fragala, J.; *et al. Angew. Chem., Int. Ed.* **2006**, *45*, 7220–7223.
65. Salaita, K.; Wang, Y. H.; Mirkin, C. A. *Nat. Nanotechnol.* **2007**, *2*, 145–155.
66. Xu, Q. B.; Rioux, R. M.; Dickey, M. D.; Whitesides, G. M. *Acc. Chem. Res.* **2008**, *41*, 1566–1577.
67. Xia, Y. N.; Whitesides, G. M. *Annu. Rev. Mater. Sci.* **1998**, *28*, 153–184.
68. Stewart, M. E.; Motala, M. J.; Yao, J.; *et al. Proc. IMechE Part N: J. Nanoeng. Nanosyst.* **2007**, *220*, 81–138.
69. Saavedra, H. M.; Mullen, T. J.; Zhang, P. P.; *et al. Rep. Prog. Phys.* **2010**, *73*, 036501.
70. Russell, M. T.; Pingree, L. S. C.; Hersam, M. C.; Marks, T. J. *Langmuir* **2006**, *22*, 6712–6718.
71. Linder, V.; Wu, H. K.; Jiang, X. Y.; Whitesides, G. M. *Anal. Chem.* **2003**, *75*, 2522–2527.
72. Li, L. J.; Fourkas, J. T. *Mater. Today* **2007**, *10*, 30–37.
73. Maruo, S.; Fourkas, J. T. *Laser Photonics Rev.* **2008**, *2*, 100–111.
74. Bhawalkar, J. D.; He, G. S.; Prasad, P. N. *Rep. Prog. Phys.* **1997**, *60*, 689.
75. Wong, S.; Deubel, M.; Perez-Willard, F.; *et al. Adv. Mater.* **2006**, *18*, 265–269.
76. Tanaka, K. *Curr. Opin. Solid State Mater. Sci.* **1996**, *1*, 567–571.
77. Takada, K.; Sun, H. B.; Kawata, S. *Appl. Phys. Lett.* **2005**, *86*, 071122-1–071122-3.
78. LaFratta, C. N.; Li, L. J.; Fourkas, J. T. *Proc. Natl. Acad. Sci. U.S.A.* **2006**, *103*, 8589–8594.
79. LaFratta, C. N.; Fourkas, J. T.; Baldacchini, T.; Farrer, R. A. *Angew. Chem., Int. Ed.* **2007**, *46*, 6238–6258.
80. Ibrahim, S.; Higgins, D. A.; Ito, T. *Langmuir* **2007**, *23*, 12406–12412.
81. Xia, Y. N.; Tien, J.; Qin, D.; Whitesides, G. M. *Langmuir* **1996**, *12*, 4033–4038.
82. Haynes, C. L.; Van Duyne, R. P. *J. Phys. Chem. B* **2001**, *105*, 5599–5611.
83. Williams, S. S.; Retterer, S.; Lopez, R.; *et al. Nano Lett.* **2010**, *10*, 1421–1428.
84. Yang, S. Y.; Ryu, I.; Kim, H. Y.; *et al. Adv. Mater.* **2006**, *18*, 709–712.
85. Gowrishankar, V.; Miller, N.; McGehee, M. D. *et al. Thin Solid Films* **2006**, *513*, 289–294.
86. Ruiz, R.; Kang, H. M.; Detcheverry, F. A.; *et al. Science* **2008**, *321*, 936–939.
87. Segalman, R. A. *Mater. Sci. Eng., R* **2005**, *48*, 191–226.
88. Han, E.; In, I.; Park, S. M.; *et al. Adv. Mater.* **2007**, *19*, 4448–4452.
89. Stoykovich, M. P.; Kang, H.; Daoulas, K. C.; *et al. ACS Nano* **2007**, *1*, 168–175.
90. Jung, Y. S.; Chang, J. B.; Verploegen, E.; *et al. Nano Lett.* **2010**, *10*, 1000–1005.
91. Hua, F.; Sun, Y. G.; Gaur, A.; *et al. Nano Lett.* **2004**, *4*, 2467–2471.
92. Kane, R. S.; Takayama, S.; Ostuni, E.; *et al. Biomaterials* **1999**, *20*, 2363–2376.
93. Zhao, X. M.; Xia, Y. N.; Schueller, O. J. A.; *et al. Sens. Actuators, A* **1998**, *65*, 209–217.
94. Grimes, A.; Breslauer, D. N.; Long, M.; *et al. Lab Chip* **2008**, *8*, 170–172.
95. Chen, C. S.; Breslauer, D. N.; Luna, J. I.; *et al. Lab Chip* **2008**, *8*, 622–624.
96. Choi, K. M. *J. Phys. Chem. B* **2005**, *109*, 21525–21531.
97. Wigenius, J.; Hamedi, M.; Inganäs, O. *Adv. Funct. Mater.* **2008**, *18*, 2563–2571.
98. Michel, B.; Bernard, A.; Bietsch, A.; *et al. IBM J. Res. Dev.* **2001**, *45*, 697–719.
99. Huang, Y.; Zhou, W.; Hsia, K.; *et al. Langmuir* **2005**, *21*, 8058–8068.
100. Jackman, R. J.; Duffy, D. C.; Cherniavskaya, O.; Whitesides, G. M. *Langmuir* **1999**, *15*, 2973–2984.
101. Kim, J. G.; Takama, N.; Kim, B. J.; Fujita, H. *J. Micromech. Microeng.* **2009**, *19*, 055017-1–055017-8.
102. Smythe, E. J.; Dickey, M. D.; Whitesides, G. M.; Capasso, F. *ACS Nano* **2009**, *3*, 59–65.
103. Odom, T. W.; Thalladi, V. R.; Love, J. C.; Whitesides, G. M. *J. Am. Chem. Soc.* **2002**, *124*, 12112–12113.
104. Truong, T. T.; Maria, J.; Yao, J.; *et al. Nanotechnology* **2009**, *20*, 434011.
105. Li, Z. W.; Gu, Y. N.; Wang, L.; *et al. Nano Lett.* **2009**, *9*, 2306–2310.

106. Lee, N. Y.; Lim, J. R.; Lee, M. J.; *et al. Langmuir* **2006**, *22*, 9018–9022.
107. Wang, P. I.; Nalamasu, O.; Ghoshal, R.; *et al. J. Vac. Sci. Technol., B* **2008**, *26*, 244–248.
108. Pla-Roca, M.; Fernandez, J.; Mills, C.; *et al. Langmuir* **2007**, *23*, 8614–8618.
109. Campos, L. M.; Truong, T. T.; Shim, D. E.; *et al. Chem. Mater.* **2009**, *21*, 5319–5326.
110. Zhang, F.; Low, H. *Nanotechnology* **2008**, *19*, 415305.
111. Svoboda, M.; Schrott, W.; Slouka, Z.; *et al. Microelectron. Eng.* **2010**, *87*, 1527–1530.
112. Yao, X.; Ito, T.; Higgins, D. A. *Langmuir* **2008**, *24*, 8939–8943.
113. Desai, S. P.; Taff, B. A.; Voldman, J. *Langmuir* **2008**, *24*, 575–581.
114. Truong, T. T.; Lin, R. S.; Jeon, S.; *et al. Langmuir* **2007**, *23*, 2898–2905.
115. Hampton, M. J.; Williams, S. S.; Zhou, Z.; *et al. Adv. Mater.* **2008**, *20*, 2667–2673.
116. Hu, Z. K.; Finlay, J. A.; Chen, L.; *et al. Macromolecules* **2009**, *42*, 6999–7007.
117. Ding, J. F.; Jiang, J.; Blanchetiere, C.; Callender, C. L. *Macromolecules* **2008**, *41*, 758–763.
118. Hu, Z.; Chen, L.; Betts, D.; *et al. J. Am. Chem. Soc.* **2008**, *130*, 14244–14252.
119. Chen, J. Y.; Mela, P.; Moller, M.; Lensen, M. C. *ACS Nano* **2009**, *3*, 1451–1456.
120. Briseno, A. L.; Mannsfeld, S. C. B.; Ling, M. M.; *et al. Nature* **2006**, *444*, 913–917.
121. Wang, C. H.; Wong, A. S.; Ho, G. W. *Langmuir* **2007**, *23*, 11960–11963.
122. Meitl, M. A.; Zhu, Z. T.; Kumar, V.; *et al. Nat. Mater.* **2006**, *5*, 33–38.
123. Kilian, K. A.; Bugarija, B.; Lahn, B. T.; Mrksich, M. *Proc. Natl. Acad. Sci. U.S.A.* **2010**, *107*, 4872–4877.
124. Mrksich, M.; Chen, C. S.; Xia, Y. N.; *et al. Proc. Natl. Acad. Sci. U.S.A.* **1996**, *93*, 10775–10778.
125. Geissler, M.; Wolf, H.; Stutz, R.; *et al. Langmuir* **2003**, *19*, 6301–6311.
126. Pagliara, S.; Persano, L.; Camposeo, A.; *et al. Nanotechnology* **2007**, *18*, 175302.
127. Jacobs, H. O.; Whitesides, G. M. *Science* **2001**, *291*, 1763–1766.
128. Cao, T. B.; Xu, Q. B.; Winkleman, A.; Whitesides, G. M. *Small* **2005**, *1*, 1191–1195.
129. Geissler, M.; McLellan, J. M.; Xia, Y. N. *Nano Lett.* **2005**, *5*, 31–36.
130. Jiang, X. R.; Bent, S. F. *J. Phys. Chem. C* **2009**, *113*, 17613–17625.
131. Shi, G.; Lu, N.; Gao, L. G.; *et al. Langmuir* **2009**, *25*, 9639–9643.
132. Xue, M. Q.; Yang, Y. H.; Cao, T. B. *Adv. Mater.* **2008**, *20*, 596–600.
133. Guan, J. J.; Chakrapani, A.; Hansford, D. J. *Chem. Mater.* **2005**, *17*, 6227–6229.
134. Jeon, S.; Menard, E.; Park, J. U.; *et al. Adv. Mater.* **2004**, *16*, 1369–1373.
135. Ahn, H.; Lee, K. J.; Childs, W. R.; *et al. J. Appl. Phys.* **2006**, *100*, 084907.
136. Xia, N.; Thodeti, C. K.; Hunt, T. P.; *et al. FASEB J.* **2008**, *22*, 1649–1659.
137. Chen, C. S.; Mrksich, M.; Huang, S.; *et al. Science* **1997**, *276*, 1425–1428.
138. Martinez, E.; Lagunas, A.; Mills, C. A.; *et al. Nanomedicine* **2009**, *4*, 65–82.
139. Lowe, A. M.; Ozer, B. H.; Wiepz, G. J.; *et al. Lab Chip* **2008**, *8*, 1357–1364.
140. Greco, P.; Cavallini, M.; Stoliar, P.; *et al. J. Am. Chem. Soc.* **2008**, *130*, 1177–1182.
141. Kwon, Y. K.; Han, J. K.; Lee, J. M.; *et al. J. Mater. Chem.* **2008**, *18*, 579–585.
142. Rolland, J. P.; Hagberg, E. C.; Denison, G. M.; *et al. Angew. Chem., Int. Ed.* **2004**, *43*, 5796–5799.
143. Jeon, N. L.; Choi, I. S.; Xu, B.; Whitesides, G. M. *Adv. Mater.* **1999**, *11*, 946–950.
144. Kim, E.; Xia, Y. N.; Zhao, X. M.; Whitesides, G. M. *Adv. Mater.* **1997**, *9*, 651–654.
145. Elhadj, S.; Rioux, R.M.; Dickey, M. D.; *et al.* **2010**, *10*, 4140–4145.
146. Hua, F.; Gaur, A.; Sun, Y. G.; *et al. IEEE Trans. Nanotechnol.* **2006**, *5*, 301–308.
147. Pokroy, B.; Epstein, A. K.; Persson-Gulda, M. C. M.; Aizenberg, J. *Adv. Mater.* **2009**, *21*, 463–469.
148. Pokroy, B.; Kang, S. H.; Mahadevan, L.; Aizenberg, J. *Science* **2009**, *323*, 237–240.
149. Chou, S. Y.; Krauss, P. R.; Renstrom, P. J. *Science* **1996**, *272*, 85–87.
150. Chou, S. Y.; Krauss, P. R.; Renstrom, P. J. *Appl. Phys. Lett.* **1995**, *67*, 3114–3116.
151. Palmieri, F.; Adams, J.; Long, B.; *et al. ACS Nano* **2007**, *1*, 307–312.
152. Costner, E. A.; Lin, M. W.; Jen, W. L.; Willson, C. G. *Annu. Rev. Mater. Res.* **2009**, *39*, 155–180.
153. Bratton, D.; Yang, D.; Dai, J. Y.; Ober, C. K. *Polym. Adv. Technol.* **2006**, *17*, 94–103.
154. Stewart, M. D.; Johnson, S. C.; Sreenivasan, S. V.; *et al. J. Microlithogr. Microfabr. Microsyst.* **2005**, *4*, 011002-1–011002-6.
155. Heath, W. H.; Palmieri, F.; Adams, J. R.; *et al. Macromolecules* **2008**, *41*, 719–726.
156. Rolland, J. P.; Maynor, B. W.; Euliss, L. E.; *et al. J. Am. Chem. Soc.* **2005**, *127*, 10096–10100.
157. Kelly, J. Y.; DeSimone, J. M. *J. Am. Chem. Soc.* **2008**, *130*, 5438–5439.
158. Zhang, H.; Nunes, J. K.; Gratton, S. E. A.; *et al. New J. Phys.* **2009**, *11*, 075018.
159. Nunes, J.; Herlihy, K. P.; Mair, L.; *et al. Nano Lett.* **2010**, *10*, 1113–1119.
160. Napier, M. E.; Desimone, J. M. *Polym. Rev.* **2007**, *47*, 321–327.
161. Gobel, O. F.; Blank, D. H. A.; ten Elshof, J. E. *ACS Appl. Mater. Interfaces* **2010**, *2*, 536–543.
162. Cavallini, M.; Albonetti, C.; Biscarini, F. *Adv. Mater.* **2009**, *21*, 1043–1053.
163. Kalima, V.; Vartiainen, I.; Saastamoinen, T.; *et al. Opt. Mater.* **2009**, *31*, 1540–1546.
164. Kang, H.; Kim, T. I.; Han, K. K.; Lee, H. H. *Org. Electron.* **2009**, *10*, 527–531.
165. Beh, W. S.; Kim, I. T.; Qin, D.; *et al. Adv. Mater.* **1999**, *11*, 1038–1041.
166. Lee, D. H.; Park, K. H.; Hong, L. Y.; Kim, D. P. *Sens. Actuators, A* **2007**, *135*, 895–901.
167. Shim, H. W.; Lee, J. H.; Kim, B. Y.; *et al. J. Nanosci. Nanotechnol.* **2009**, *9*, 1204–1209.
168. Dickey, M. D.; Lipomi, D. J.; Bracher, P. J.; Whitesides, G. M. *Nano Lett.* **2008**, *8*, 4568–4573.
169. Huang, T. C.; Chan, B. D.; Ciou, J. K.; Yang, S. Y. *J. Micromech. Microeng.* **2009**, *19*, 015018-1–015018-6.
170. Mazzoldi, A.; Tesconi, M.; Tognetti, A.; *et al. Mater. Sci. Eng. C, Biomimetic Supramolecular Syst.* **2008**, *28*, 1057–1064.
171. Lee, J. N.; Park, C.; Whitesides, G. M. *Anal. Chem.* **2003**, *75*, 6544–6554.
172. Shir, D. J.; Jeon, S.; Liao, H.; *et al. J. Phys. Chem. B* **2007**, *111*, 12945–12958.
173. Paul, K. E.; Breen, T. L.; Hadzik, T.; *et al. J. Vac. Sci. Technol., B* **2005**, *23*, 918–925.
174. Aizenberg, J.; Rogers, J. A.; Paul, K. E.; Whitesides, G. M. *Appl. Opt.* **1998**, *37*, 2145–2152.
175. Aizenberg, J.; Rogers, J. A.; Paul, K. E.; Whitesides, G. M. *Appl. Phys. Lett.* **1997**, *71*, 3773–3775.
176. Yin, Y. D.; Gates, B.; Xia, Y. N. *Adv. Mater.* **2000**, *12*, 1426–1430.
177. Paul, K. E.; Zhu, C.; Love, J. C.; Whitesides, G. M. *Appl. Opt.* **2001**, *40*, 4557–4561.
178. Lee, J.; Hasan, W.; Stender, C. L.; Odom, T. W. *Acc. Chem. Res.* **2008**, *41*, 1762–1771.
179. Henzie, J.; Barton, J. E.; Stender, C. L.; Odom, T. W. *Acc. Chem. Res.* **2006**, *39*, 249–257.
180. Jeon, S.; Shir, D. J.; Nam, Y. S.; *et al. Opt. Express* **2007**, *15*, 6358–6366.
181. Shir, D.; Nelson, E. C.; Chen, Y. C.; *et al. Appl. Phys. Lett.* **2009**, *94*, 011101.
182. Ramanan, V.; Nelson, E.; Brzezinski, A.; *et al. Appl. Phys. Lett.* **2008**, *92*, 173304-1–173304-3.
183. Shir, D.; Liao, H. W.; Jeon, S.; *et al. Nano Lett.* **2008**, *8*, 2236–2244.
184. George, M. C.; Nelson, E. C.; Rogers, J. A.; Braun, P. V. *Angew. Chem., Int. Ed.* **2009**, *48*, 144–148.
185. Lipomi, D. J.; Martinez, R. V.; Rioux, R. M.; *et al. ACS Appl. Mater. Interfaces* **2010**, *2*, 2503–2514.
186. Lipomi, D. J.; Chiechi, R. C.; Dickey, M. D.; Whitesides, G. M. *Nano Lett.* **2008**, *8*, 2100–2105.
187. Lipomi, D. J.; Ilievski, F.; Wiley, B. J.; *et al. ACS Nano* **2009**, *3*, 3315–3325.
188. Xu, Q. B.; Bao, J. M.; Capasso, F.; Whitesides, G. M. *Angew. Chem., Int. Ed.* **2006**, *45*, 3631–3635.
189. Liu, H. Q.; Kameoka, J.; Czaplewski, D. A.; Craighead, H. G. *Nano Lett.* **2004**, *4*, 671–675.
190. Xue, M. Q.; Zhang, Y.; Yang, Y. L.; Cao, T. B. *Adv. Mater.* **2008**, *20*, 2145–2150.
191. Liu, H. Q.; Reccius, C. H.; Craighead, H. G. *Appl. Phys. Lett.* **2005**, *87*, 253106.
192. McCullough, R. D. *Adv. Mater.* **1998**, *10*, 93–116.
193. Wu, D. M.; Fang, N.; Sun, C.; *et al. Appl. Phys. Lett.* **2003**, *83*, 201–203.
194. Cubukcu, E.; Yu, N. F.; Smythe, E. J.; *et al. IEEE J. Sel. Top. Quantum Electron.* **2008**, *14*, 1448–1461.
195. Kneipp, K.; Kneipp, H.; Itzkan, I.; *et al. J. Phys.: Condens. Matter* **2002**, *14*, R597–R624.
196. Valentine, J.; Zhang, S.; Zentgraf, T.; *et al. Nature* **2008**, *455*, 376–379.
197. Liu, N.; Guo, H. C.; Fu, L. W.; *et al. Nat. Mater.* **2008**, *7*, 31–37.
198. Klar, T. A.; Kildishev, A. V.; Drachev, V. P.; Shalaev, V. M. *IEEE J. Sel. Top. Quantum Electron.* **2006**, *12*, 1106–1115.
199. Lipomi, D. J.; Kats, M. A.; Kim, P.; *et al. ACS Nano* **2010**, *4*, 4017–4026.
200. Lucotti, A.; Zerbi, G. *Sens. Actuators, B* **2007**, *121*, 356–364.
201. Sharma, A. K.; Jha, R.; Gupta, B. D. *IEEE Sens. J.* **2007**, *7*, 1118–1129.
202. Leung, A.; Shankar, P. M.; Mutharasan, R. *Sens. Actuators, B* **2007**, *125*, 688–703.
203. Guieu, V.; Talaga, D.; Servant, L.; *et al. J. Phys. Chem. C* **2009**, *113*, 874–881.
204. Smythe, E. J.; Dickey, M. D.; Bao, J. M.; *et al. Nano Lett.* **2009**, *9*, 1132–1138.
205. Lipomi, D. J.; Martinez, R. V.; Kats, M. A.; *et al. Nano Lett.*, **2011**, *11*, 632–636.

Biographical Sketches

Darren J. Lipomi was born in Rochester, New York, in 1983. He earned his BA in chemistry, with a minor in physics, from Boston University in 2005. Under Prof. James S. Panek, his research focused on the total synthesis of natural products and asymmetric reaction methodology. He earned his AM and PhD in chemistry at Harvard University in 2008 and 2010, with Prof. George M. Whitesides. At Harvard, he developed several unconventional approaches to fabricate micro- and nanostructures for electronic and optical applications. He is now an Intelligence Community Postdoctoral Fellow in the Department of Chemical Engineering at Stanford University.

Ramsés V. Martínez was born in Madrid in 1981. He completed his Bachelor's and Master's degrees in physics at Universidad Autónoma de Madrid in June 2004. In 2009, He received his PhD degree from the Spanish High Council of Scientific Research (CSIC) under the supervision of Prof. R. García. He is currently a postdoctoral researcher in Prof. George M. Whitesides' group at Harvard University. His current research focuses on the development of new simple and low-cost methods of nanofabrication.

Ludovico Cademartiri obtained a Laurea degree in Materials Science (cum laude) from the University of Parma in 2002 and a PhD in Chemistry from the University of Toronto in 2008. He is currently a NSERC Postdoctoral Fellow in the group of George M. Whitesides at Harvard University. His research is recognized by national and international awards (e.g. ACS Young Investigator Award, MRS Graduate Student Award, CSC Prize for Graduate Work in Inorganic Chemistry, the Governor General Gold Medal). Starting January 2012 he will be Assistant Professor in the Department of Materials Science & Engineering of Iowa State University.

George M. Whitesides received his A.B. degree from Harvard University in 1960 and his PhD degree from the California Institute of Technology in 1964. A Mallinckrodt Professor of Chemistry from 1982 to 2004, he is now a Woodford L. and Ann A. Flowers University Professor. Prior to joining the Harvard faculty, he was a member of the chemistry faculty of the Massachusetts Institute of Technology. His research interests include physical and organic chemistry, materials science, biophysics, complexity, surface science, microfluidics, self-assembly, micro- and nanotechnology, and cell-surface biochemistry.